Upgrade of the PADME experiment for the X17 Search

Mario Antonelli for the PADME Collaboration

Search for X17 resonance

ATOMKI Collaboration observed anomalies in the angular correlation of e^+e^- pairs emitted via internal pair conversion in the ^{8}Be, ^{4}He and ^{12}C nuclear de-excitation

→ results compatible with a new neutral mediator called X17

Vector coupling

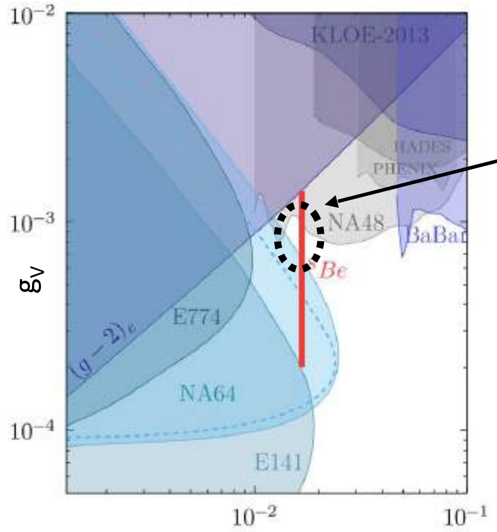

Phys. Rev. D101, 071101

Pseudo-scalar coupling

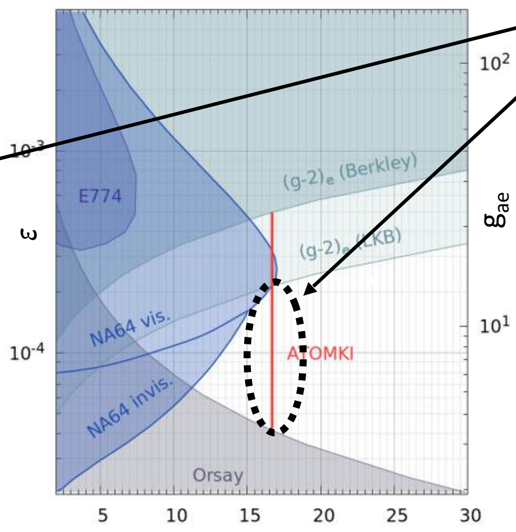

Phys. Rev. D104, L111102

There is still room in the phase space for New Physics interpretation!

Resonant search on fixed target

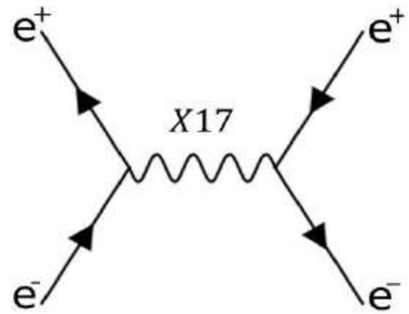

e^+e^- annihilation is the main production process

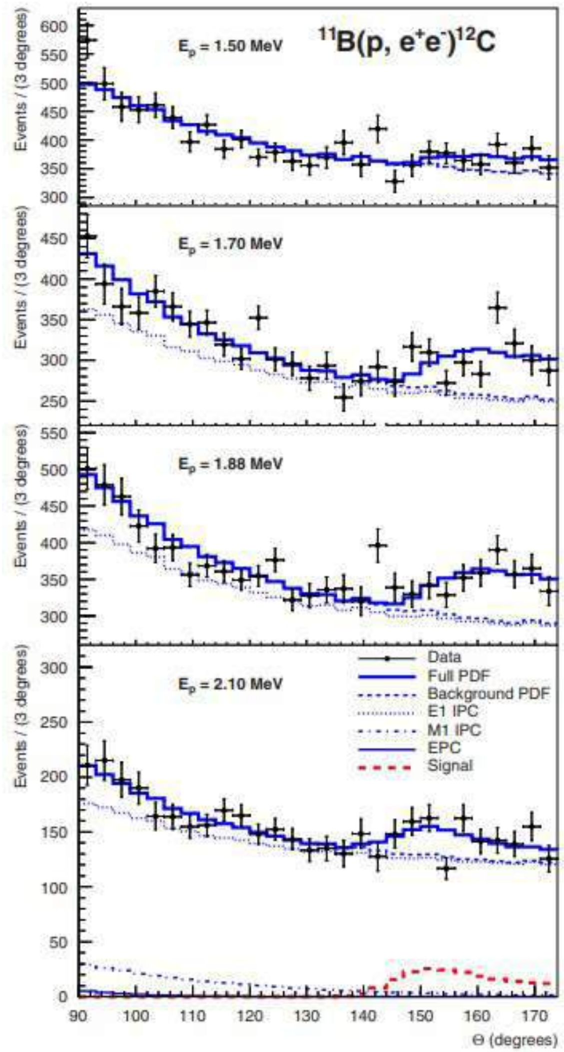

PADME measurement idea: perform a very fine scan of √s around the hypothetical mass resonance using positron beam with E_{beam} ~ 283 MeV on target → measure a 2-body final state

PADME Experiment in Run III

Experimental setup

- Active target polycrystalline diamond
- ECal: 616 BGO crystals, each 21x21x230 mm^3
- ETagger (scintillator detector) in front of ECal for e/γ discrimination
- TimePix3 high granularity silicon-based detector for beam spot
- LeadGlass luminometer (NA62 Large Angle Veto spare block)

Elements not used: charged particle veto and magnetic field (residual 12.5 G)

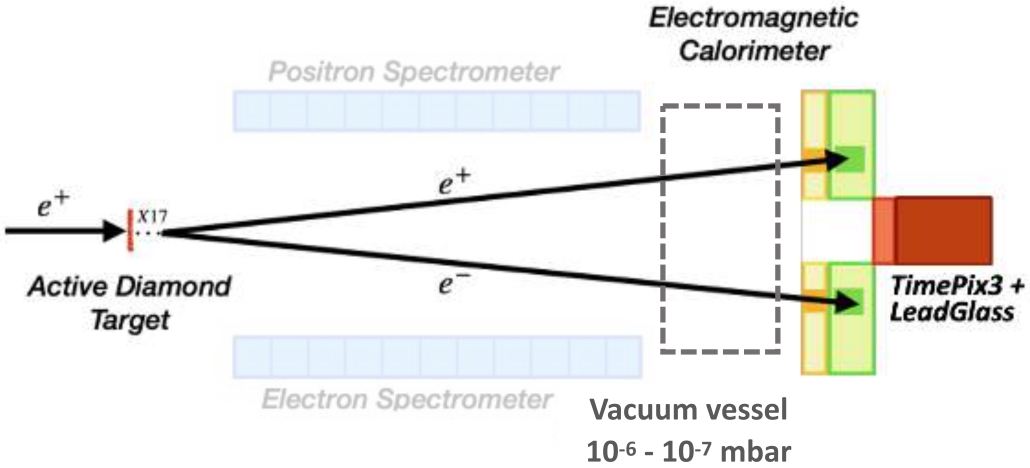

Run III Dataset ~ $6x10^{11}$ PoT (~10^{10} PoT per $\sqrt{s}$ point)

- 42 on-resonance points in 2 scans: E_{beam} @(263, 299) MeV ($\sqrt{s}$ steps of ~20 keV)
- 6 out-of-resonance points: X17 production forbidden
  - 5 points with ~ 10^{10} PoT each and E_{beam} @(205, 211) MeV
  - 1 point with ~ $2x10^{10}$ PoT and E_{beam} = 402 MeV

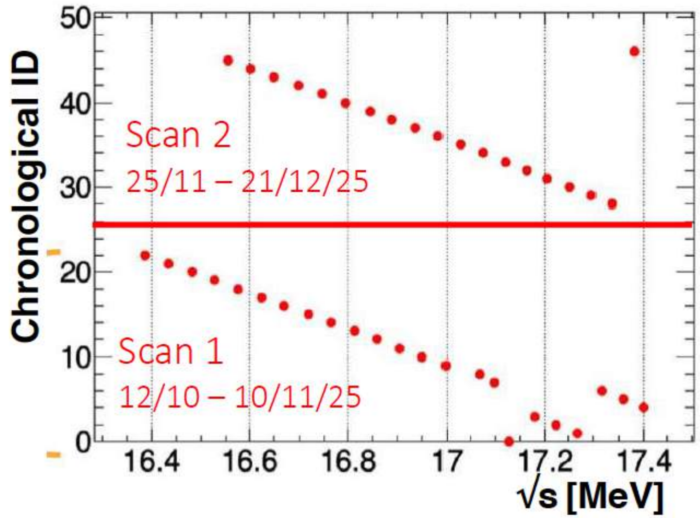

Run III Analysis Strategy

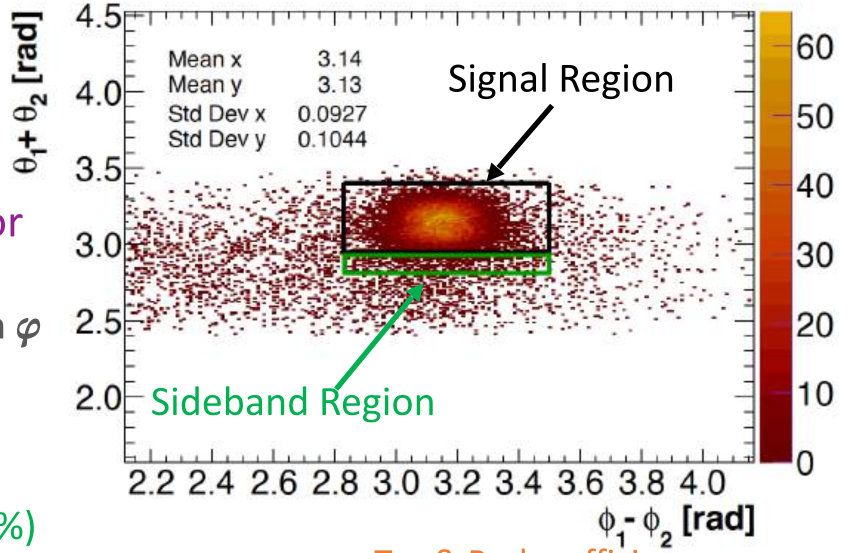

N_2: selection algorithm as independent as possible on beam and detector conditions: required 2 clusters in ECal

- Acceptance reduced by 30% due the presence of the magnet → Cut regions in φ
- $\phi 1 - \phi 2$ vs $\theta 1 + \theta 2$ cut in the center of mass to define the signal region

  → Signal Region is 3σ around the mean value

  → Sideband Region for Bremsstrahlung background normalization (~ 4%)

Tag & Probe efficiency

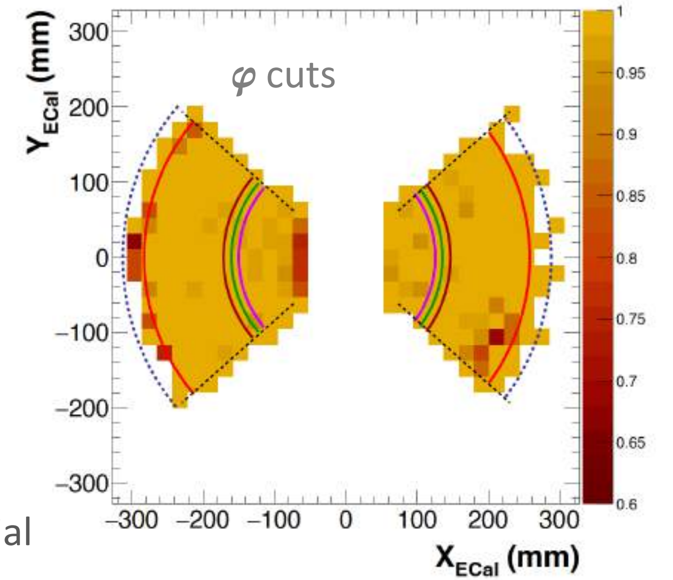

B: main backgrounds are Bhabha(irreducible) and $\gamma\gamma$ annihilation.

- The expected background yield per PoT is determined with MC and reconstruction efficiency estimated with Tag&Probe method → data/MC compatible with 1
- B yield normalized to below-resonance energy points to improve systematic uncertainty
- Radiative corrections e+e-(γ) and $\gamma\gamma(\gamma)$ evaluated using BabaYaga

N_{PoT}: The number of positron on target per bunch is determined using the LeadGlass calorimeter charge.

$$N_{PoT} = \frac{Q_{LG}}{Q_{1e^+,402\,[MeV]}} \times \frac{402}{E_{beam}[MeV]}$$

- Estimation corrected for radiation induced loss and the energy loss in the passive material

Run III Analysis Strategy

S: the width of the expected excess receive contributions by the beam energy spread and from the electron motion in the target.

- Convolution of the Gaussian for the BES with a Lorentzian

ε_{Sig} : signal efficiency determined from MC

- Use of the ratio ε_{Sig}/B significantly reduces detector-related systematic

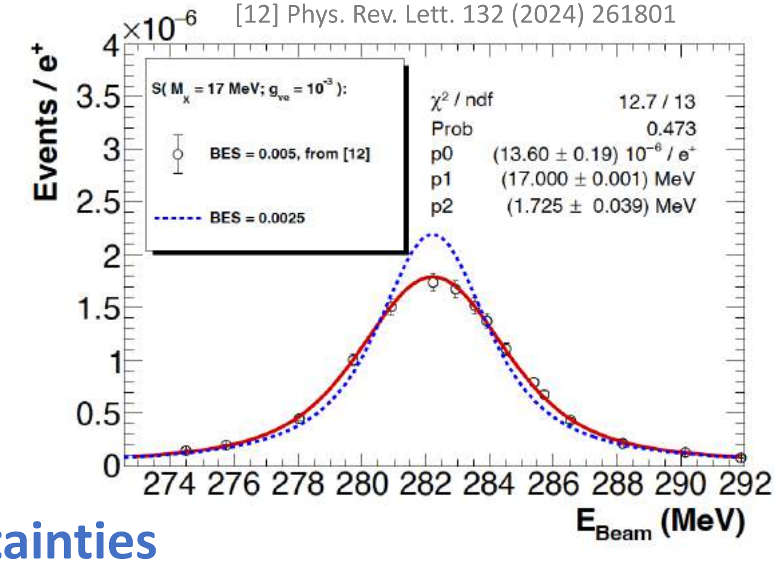

Summary of the systematic uncertainties

Uncorrelated errors	
Source	Uncertainty (% per energy point)
$N_2(s)$	0.60
$B(s)$	0.54
$N_{\mathrm{PoT}}(s)$	0.35
Total on $g_R(s)$	0.88
$K(s)$, constant term	
Source	Uncertainty (%)
Lead-glass calibration	2.0
Absolute B yield	1.8
Energy-loss correction to N_{PoT}	0.5
Radiation-induced correction to N_{PoT}	0.3
Total	2.8
$K(s)$, $\sqrt{s}$-slope	
Source	Expected value (%/MeV)
Radiative corrections	$-0.6 \pm 0.2 \pm 0.6$
Total	-0.6 ± 0.6

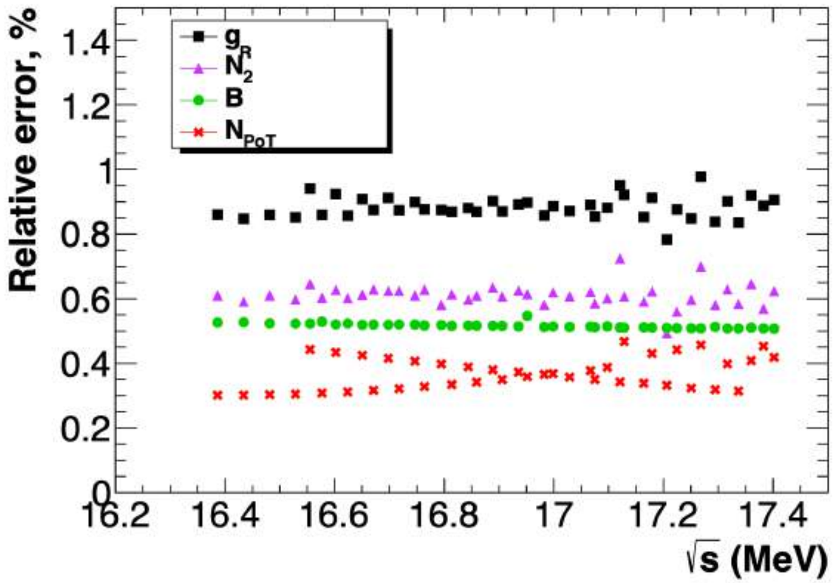

Run III Results

Blind - unbliding procedure

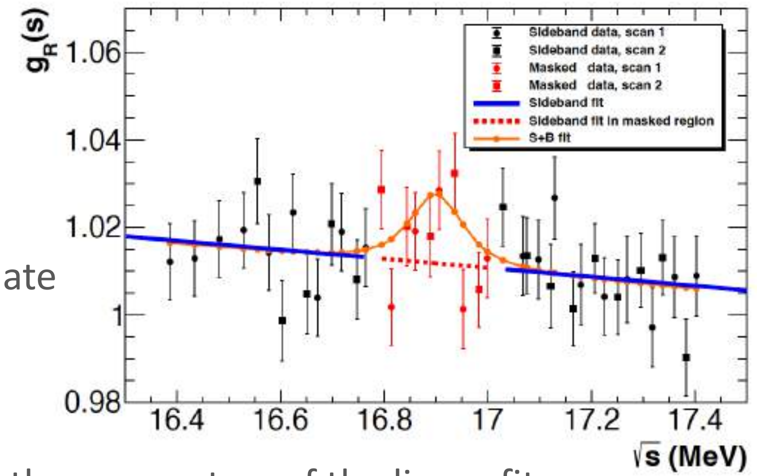

Large expected X17 mass resolution → no sideband region in √s can be defined to validate the statistical approach → Validation procedure described in 2503.05650 were used

- Aim to blindly define a sideband in gR(s), excluding 10 periods of the scan
- Define the masked periods by optimizing the probability of a linear fit in s

Data validation criteria are based on the fit quality, the distribution of the fit pulls, and the parameters of the linear fit

Statistical treatment

Test statistic based on Likelihood ratio between S+B and B-only and includes terms for each nuisance parameter

- For a given M_X, $CL_s = \dfrac{P_S}{(1-P_B)}$ is used to define the upper limit on g_{ve}

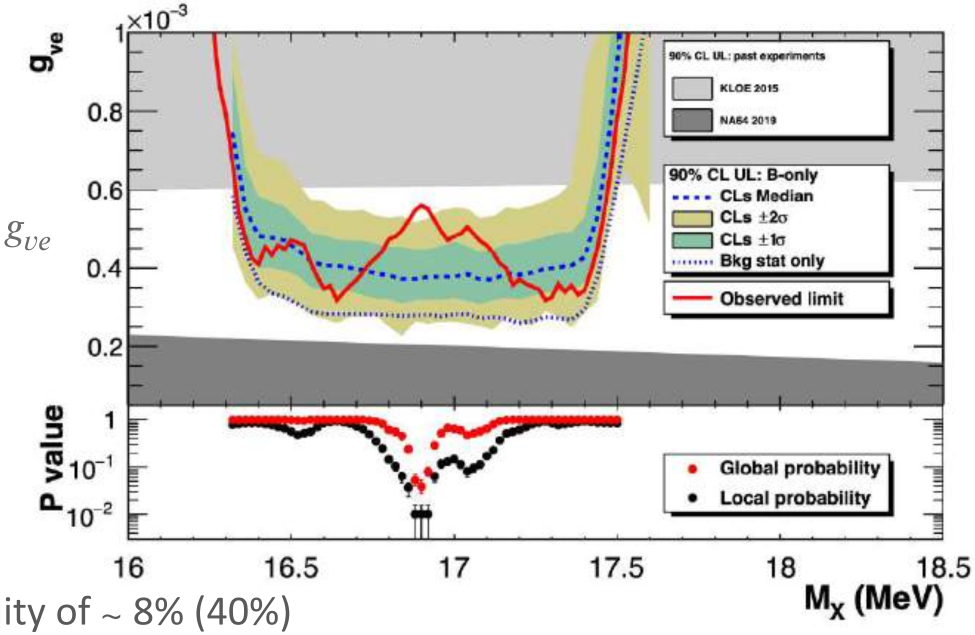

Run III Results

Excess observed, 2.5 σ local, 1.8(2) σ global significance

corresponding to mass $M_X = 16.9\ MeV$ and a coupling

$g_{ve} = 5 \times 10^{-4}$

Second excess present at $M_X \cong 17.1\ MeV$, with a local (global) probability of ~ 8% (40%)

Run III Results

Blind - unbliding procedure

Large expected X17 mass resolution → no sideband region in √s can be defined to validate the statistical approach → Validation procedure described in 2503.05650 were used

- Aim to blindly define a sideband in gR(s), excluding 10 periods of the scan
- Define the masked periods by optimizing the probability of a linear fit in s

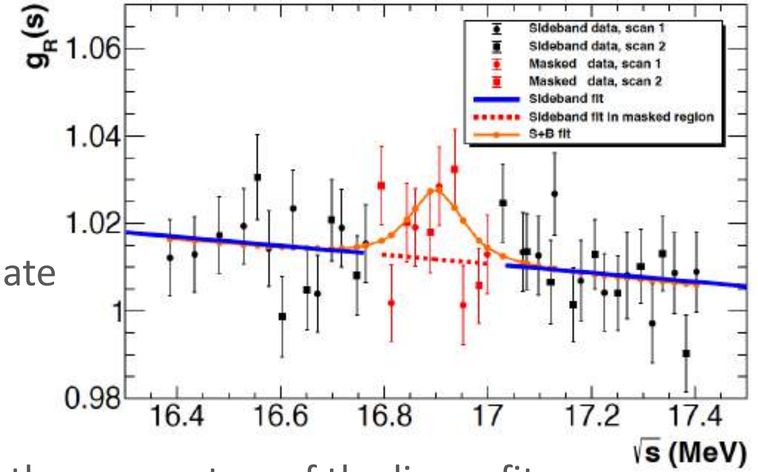

Data validation criteria are based on the fit quality, the distribution of the fit pulls, and the parameters of the linear fit

Statistical treatment

Test statistic based on Likelihood ratio between S+B and B-only and includes terms for each nuisance parameter

- For a given M_X, $CL_s = \frac{P_S}{(1-P_B)}$ is used to define the upper limit on g_{ve}

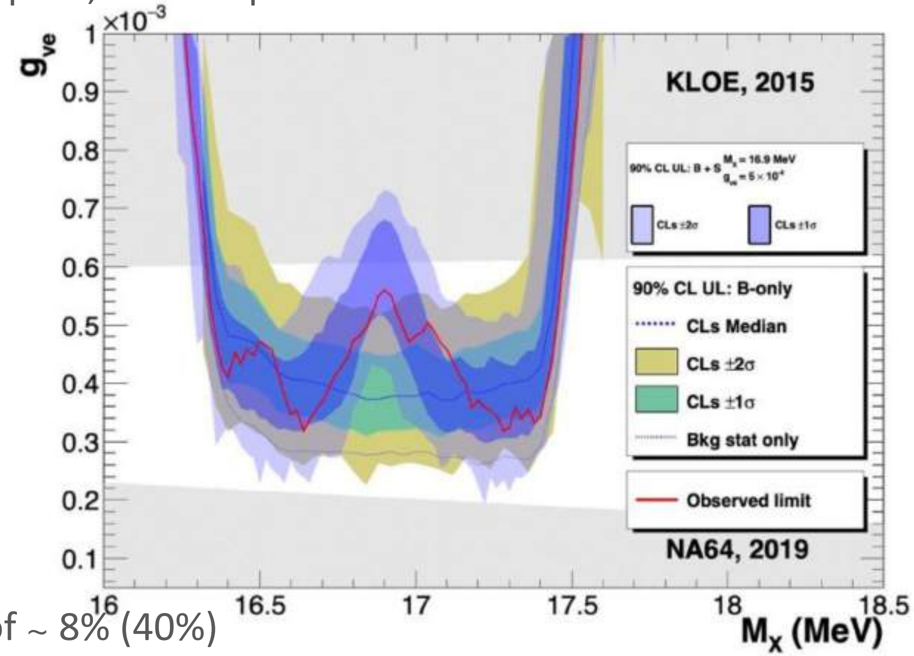

Run III Results

Excess observed, 2.5 σ local, 1.8(2) σ global significance

corresponding to mass $M_X = 16.9\ MeV$ and a coupling

$$g_{ve} = 5 \times 10^{-4}$$

Second excess present at $M_X \cong 17.1\ MeV$, with a local (global) probability of ~ 8% (40%)

PADME Upgrade for Run IV

The goal of Run IV is to increase sensibility to confirm/disprove Run III result

- Diamond target position moved downstream by ~30 cm + position readout changed
- Passive material removed and PADME Magnet fully degaussed
- Radiation loss monitor system for online LG calibration

- New detectors
  - PadMMe Micromegas chamber replaced the ETagger
  - TMM Micromegas replace the TimePix beam monitor

Diamond target moved

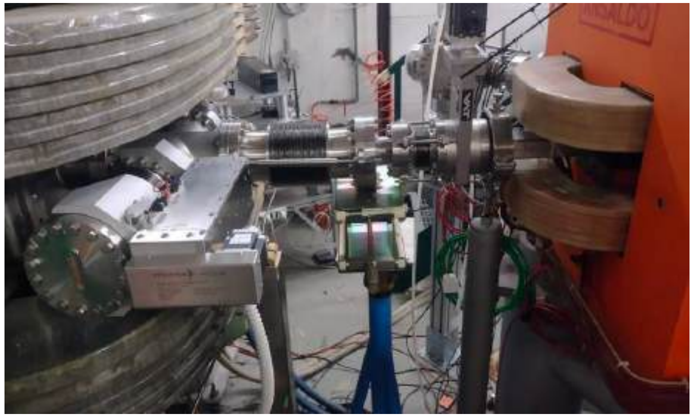

PadMMe

TMM

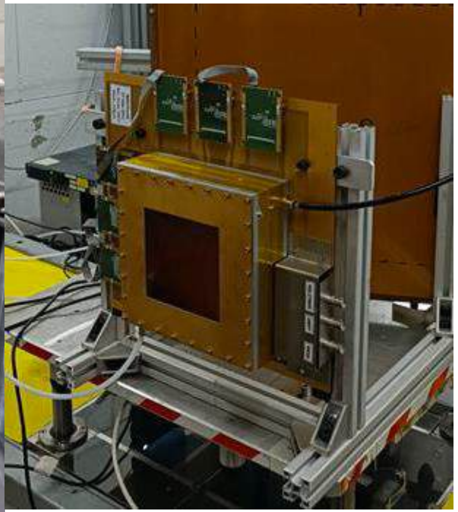

Source	Uncertainty		Improvement
	Run III	Run IV	
N_2	0.6	0.3	New target position → **acceptance increased**
B	0.54	0.3	PadMMe → **ee/$\gamma\gamma$ discrimination** + angular-momentum resolution increasing
N_{PoT}	0.35	0.3	**3 different beam spot monitor** (Target-PadMMe-TMM) + **online LG calibration system**
Total	**0.88**	**0.5**	

PADME MICROMEGAS detector

The **padMMe** detector is a **floating mesh resistive anode Micromegas detector**, placed in front of ECAL.

The **active area is 65x65 cm^2**, with **two drift gaps of 5 cm** and two amplification gaps of 128 μm, each with a dedicated readout plane with **strips on both coordinates**.

The readout panel is made of FR4 - Honeycomb Nomex - FR4 sandwich glued to the PCBs.

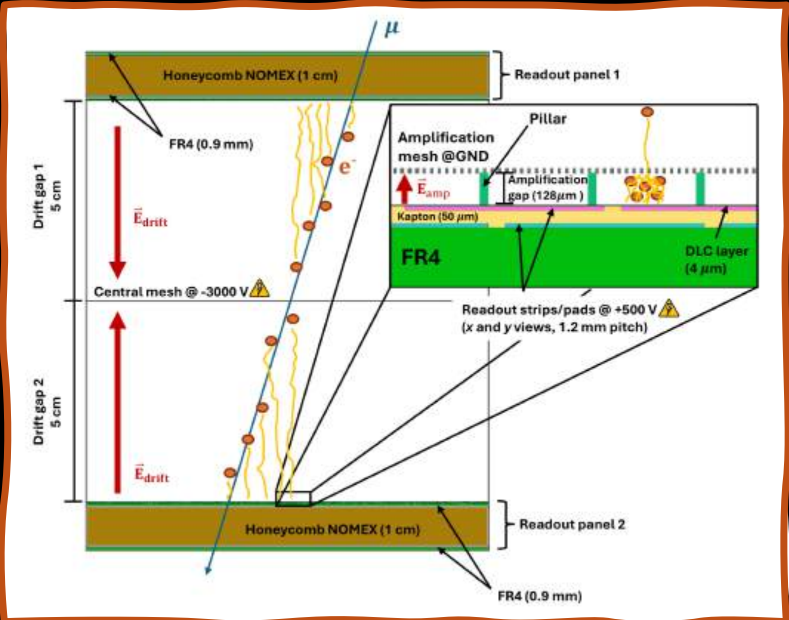

The three meshes have stainless steel wires (18 μm of diameter, grid pitch of 45 μm)

The gas mixture is $\mathbf{Ar}:\mathbf{C}F_4:iC_4H_{10}$ = **88:10:2**

→ drift velocity = 10.5 $cm/\mu s$

→ ~100 total ionizations/cm

padMMe: pcb design

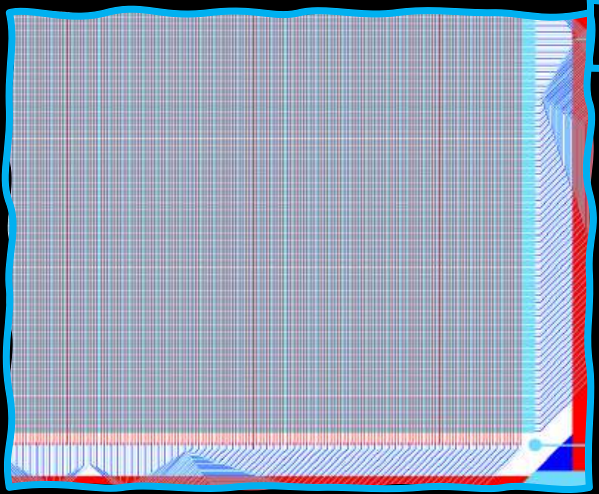

Straight strips

The x and y coordinates each are read by parallel Copper strips, separated by 1.2 mm pitch, which guarantee a spatial resolution of ~ 300µm on the layer facing the amplification gap.

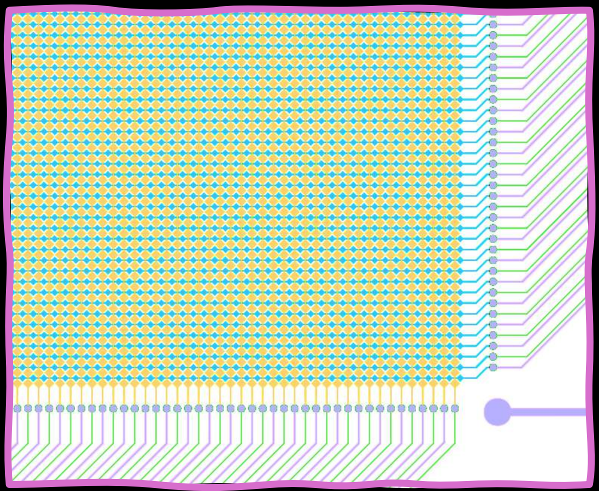

Rhomboidal strips

The reading layers are composed of rhomboidal shaped strips, always with a pitch of 1.2 mm. The two layers are shifted one to the other in such a way as not to overlap the x and y readout pads. This technology minimizes the capacitive coupling between the two layers, keeping the resolution on each coordinate of ~ 300 µm. The pads have different areas, 0.49 mm^2 for the upper layer and 0.25 mm^2 for the down layer, making the capacitive coupling to the resistive layer the same for both the readout layers. Anyway, such difference in surfaces of the pads causes a difference of ~ 20% for the collected charge of the two layers.

padMMe: readout features

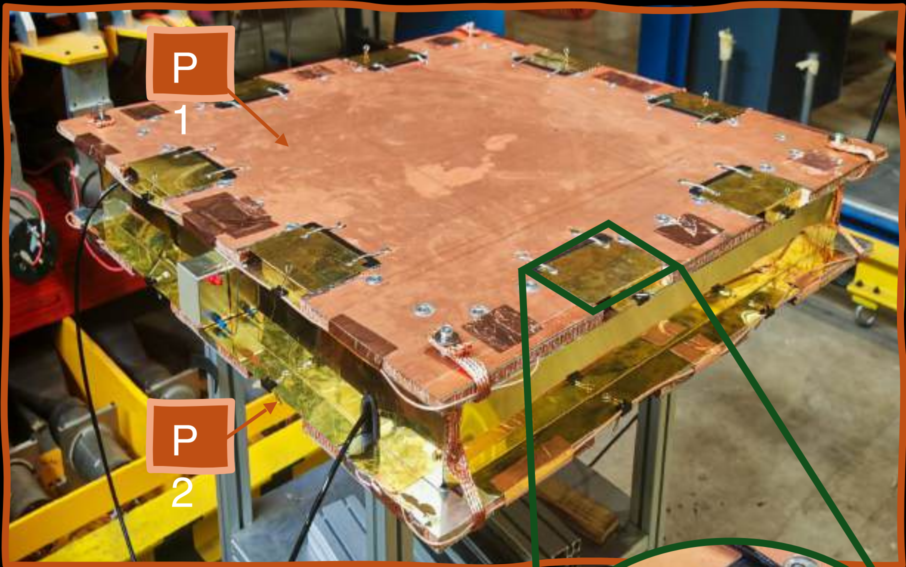

- 512 channels for each side → **2048 channels for readout plane.**
- Every 128 channels read out by one **APV25 chip**
- Each APV25 is connected to the Front-End Card for event building.

Rhomboidal strips

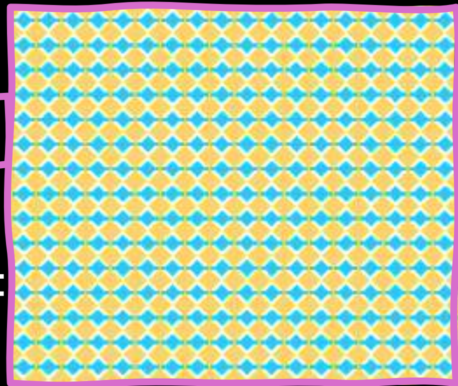

Two different segmentation layout tested:
- **straight strips**
- **rhomboidal strips**

→Same **pitch of 1.2 mm** (X, Y readout) → $\sigma_{X,Y} \sim$ **300 μm**

→Expected Z-resolution **~ 1-2 mm**.

Rhomboidal strips now in PADME

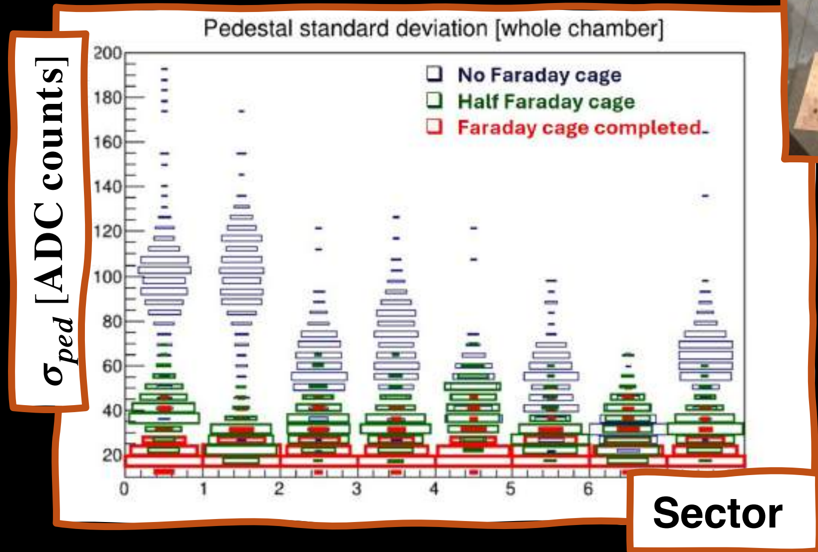

We improved the grounding and shielding of the chamber by a Faraday cage → **Electronic noise largely suppressed**

HV features

Readout panel is made of **two separate PCB** glued together → hole of 7.2 mm. Strip segmentation is adapted to have **4 quadrants** for the whole panel.

The PCBs have **separate HV regions**, to enable operation in the beam region:

- An **inner circle** (R = 6 cm) → **low gain**
- A **middle ring** (ΔR = 4 cm) → **low gain**
- An **external zone** → **gain** $\sim 10^4$

The nominal readout voltage:

- Inner circle → 350 V
- Middle ring → 350 V
- External zone → 490 V

The drift voltage is -3000 V

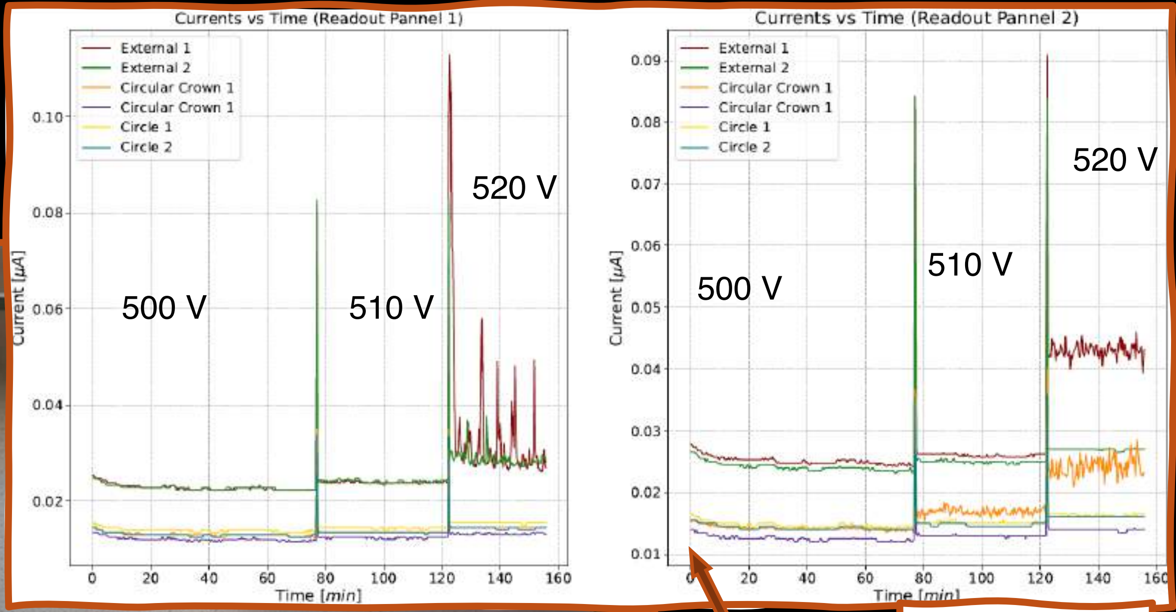

Time

The discharges at high readout HV are reduced thanks to the resistive layer.

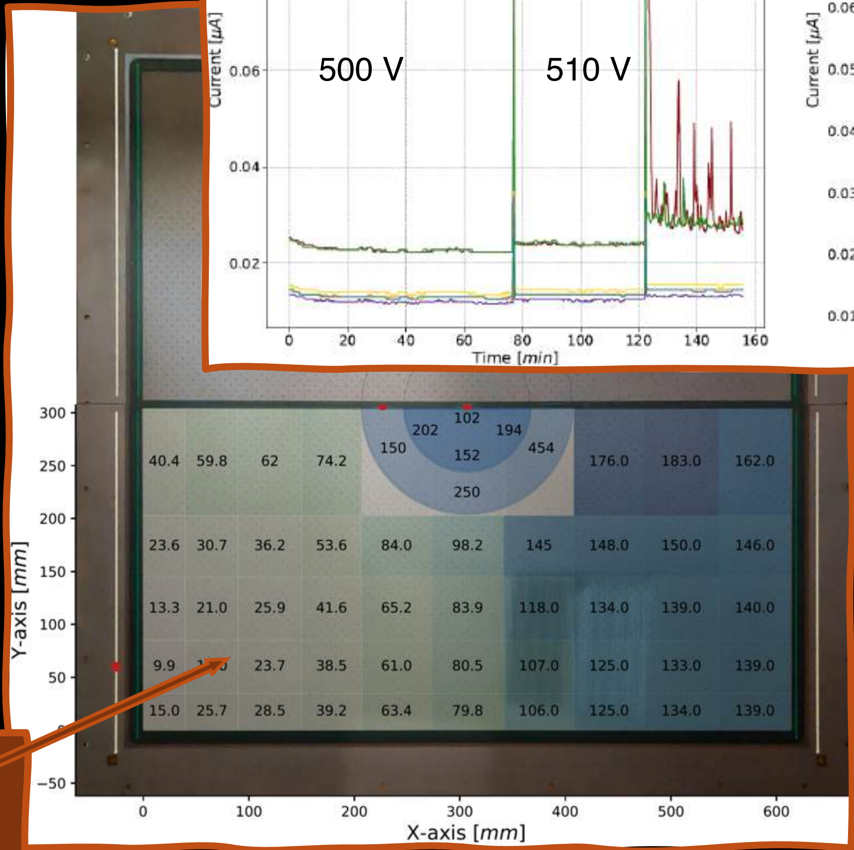

Resistance map [MΩ]

HV features

Readout panel is made of **two separate PCB** glued together → hole of 7.2 mm. Strip segmentation is adapted to have **4 quadrants** for the whole panel.

The PCBs have **separate HV regions**, to enable operation in the beam region:

- An **inner circle** (R = 6 cm) → **low gain**
- A **middle ring** ($\Delta R = 4$ cm) → **low gain**
- An **external zone** → **gain** $\sim 10^4$

The nominal readout voltage:

- Inner circle → 350 V
- Middle ring → 350 V
- External zone → 490 V

The drift voltage is -3000 V

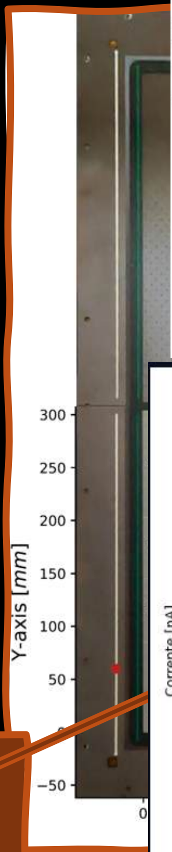

Resistance map [MΩ]

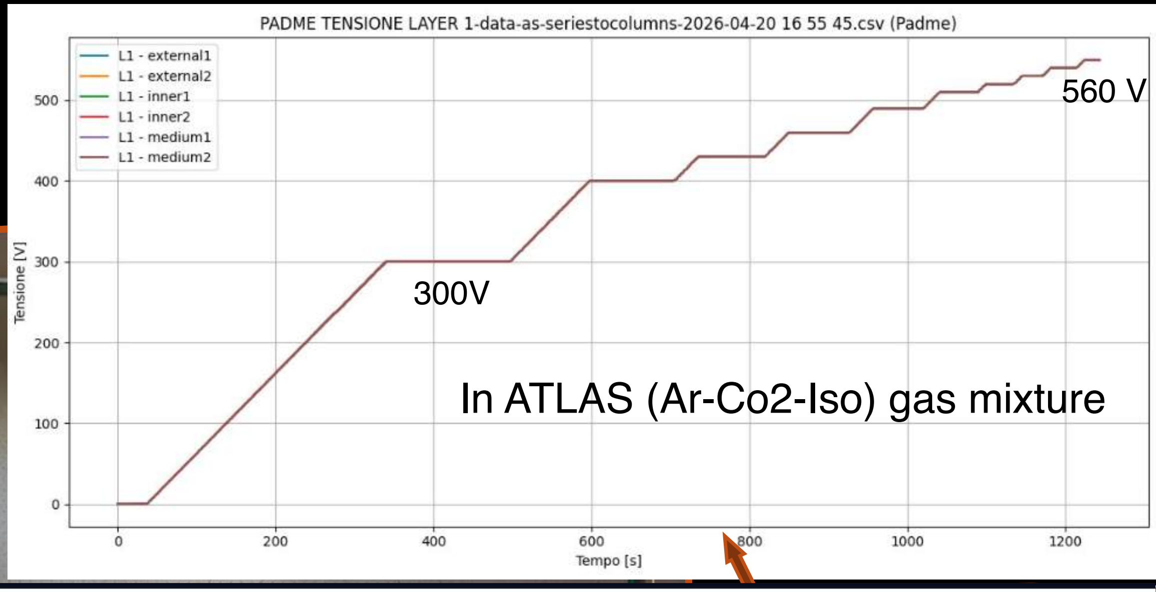

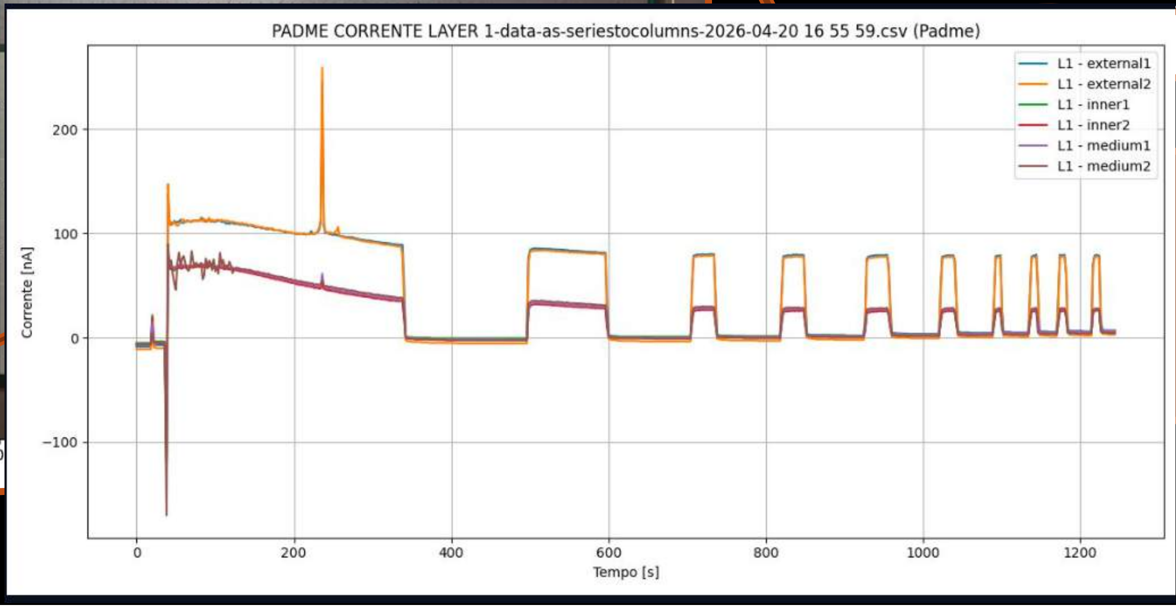

padMMe: Front End & DAQ

PADME INFN LNF

- APV25s are integrated in the Scalable Readout System which includes Front-End Cards.
- APV25 has → **200 ns charge integrator**
  → **50 ns CR-RC shaper.**
  → **Analog signal sampled at 40 MHz (25 ns).**

- **The padMMe DAQ window is 675 ns.**
- The DAQ software is mmDAQ3
  → includes online monitor feature

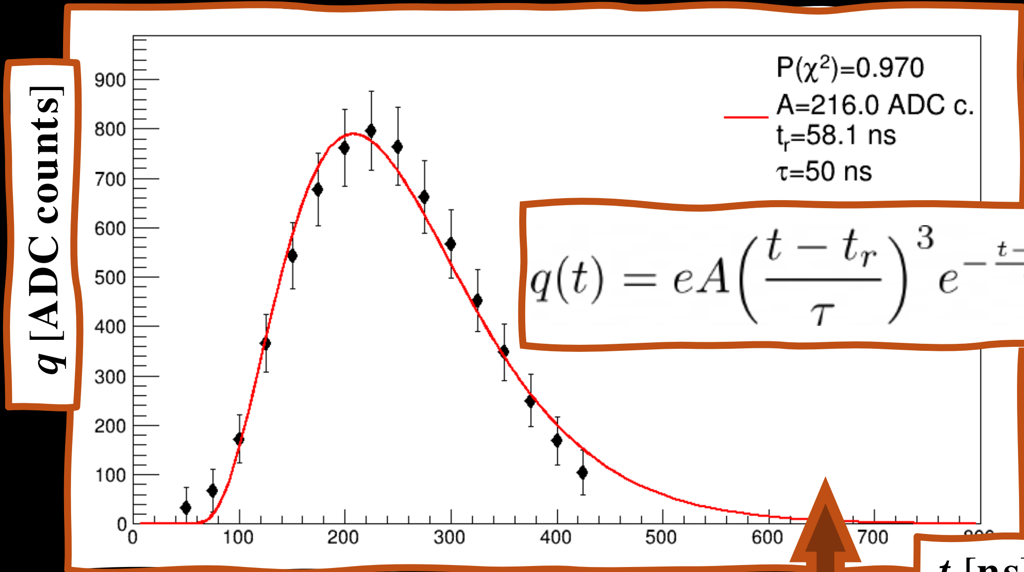

$$q(t) = eA\left(\frac{t-t_r}{\tau}\right)^3 e^{-\frac{t-t_r}{\tau}}$$

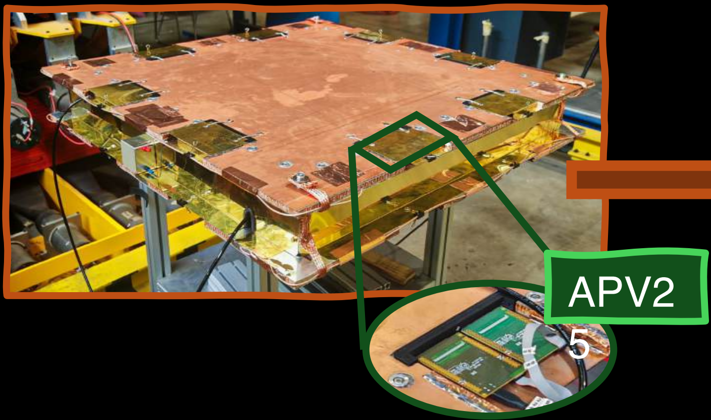

padMMe: collected charge spectrum

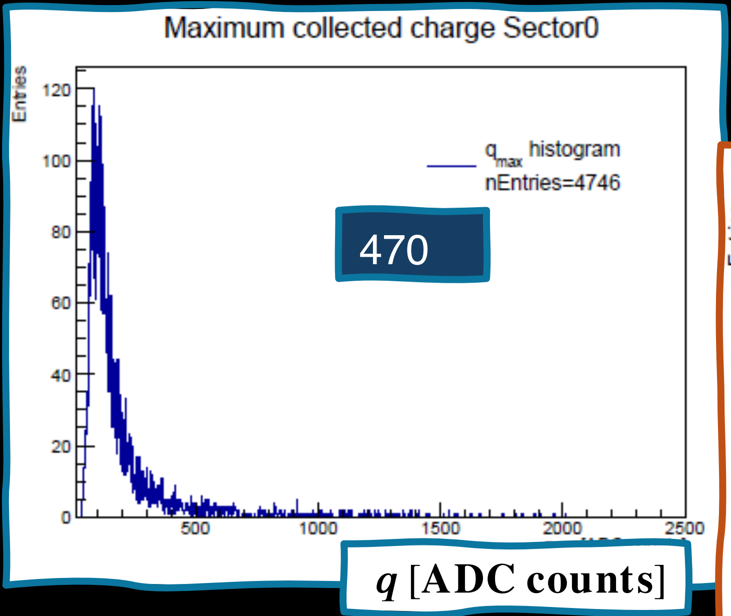

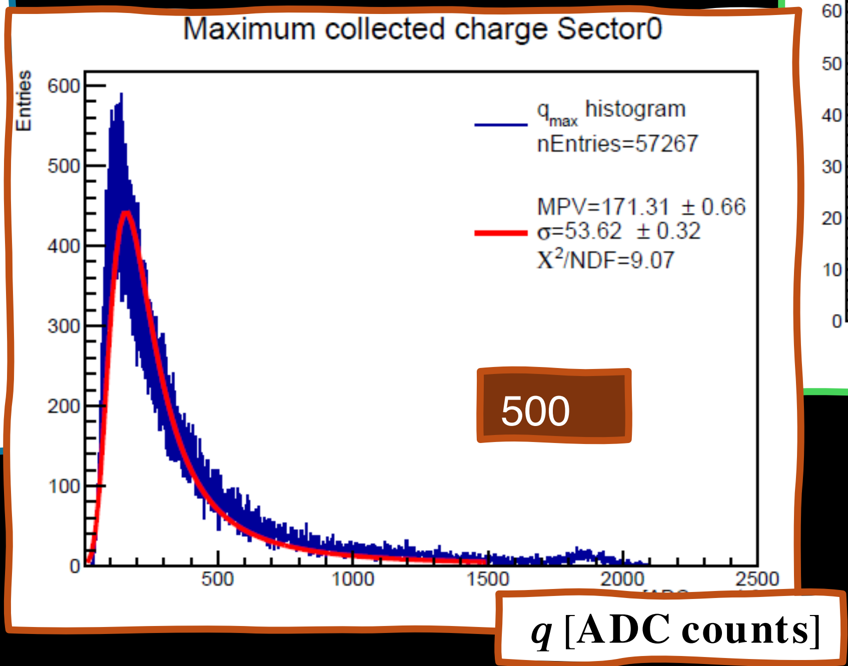

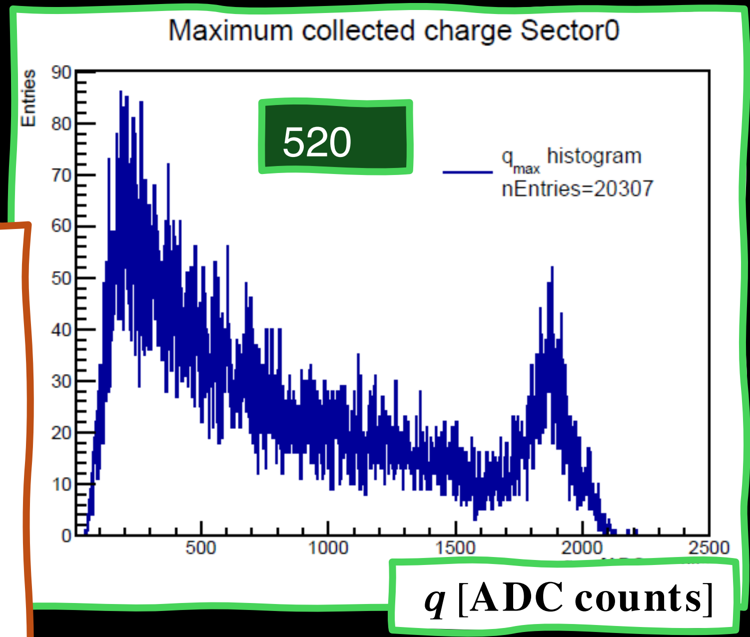

padMMe @ Cosmic Rays Stand

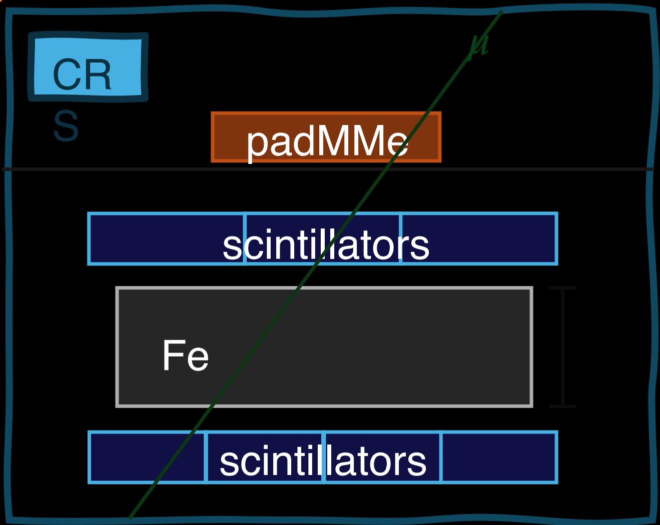

The padMMe was first tested and validated at the **Cosmic Rays Stand at LNF**, using cosmic rays, triggering with two sets of scintillators.

❖ Study **padMMe response vs readout HV**, to determine the HV work point:
- ➢ measure of the **first Townsend coefficient** α
  - → determination of **gain**
- ➢ **hit efficiencies,** ϵ_{hit}

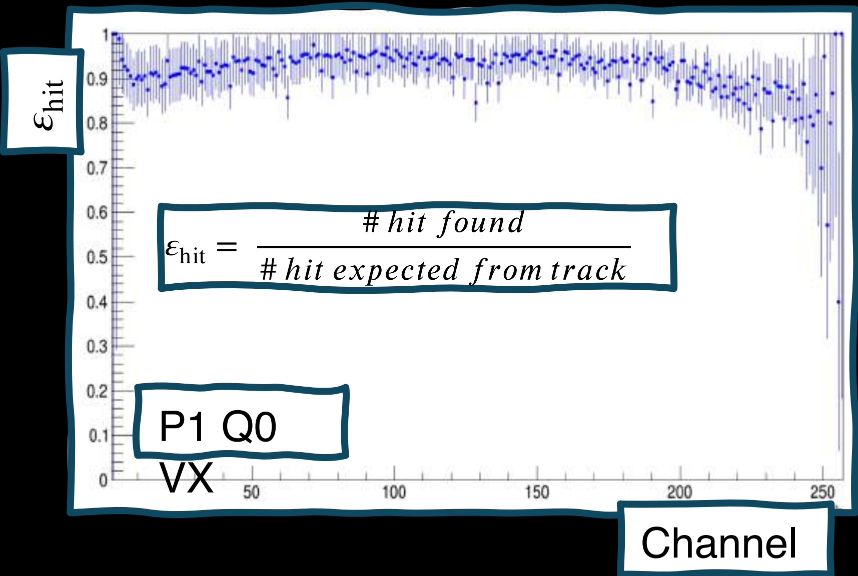

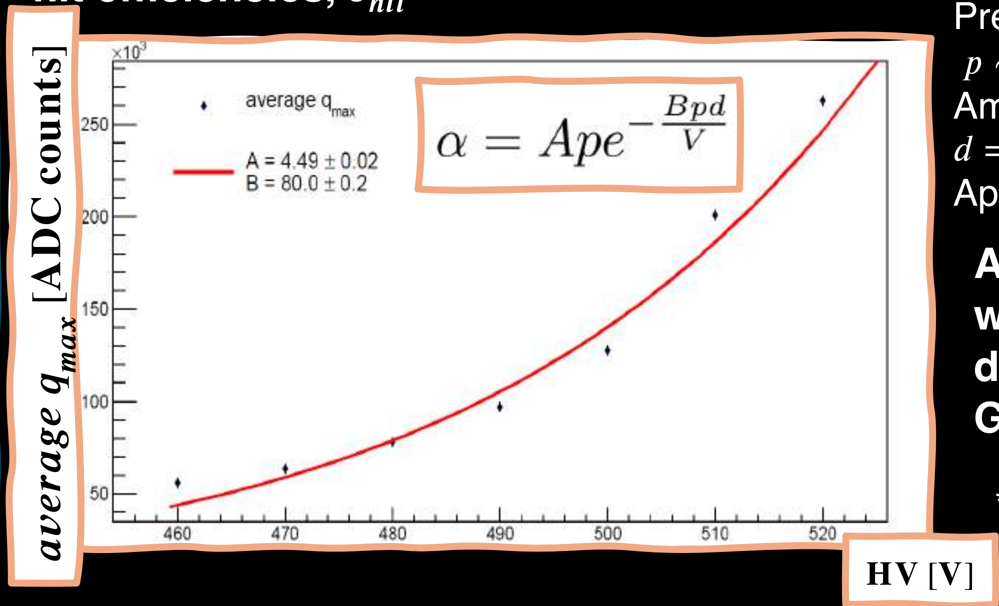

Pressure:
$p \sim 1\ bar * \sim 750$ mmHg
Amplification gap:
$d = 128$ μm
Applied voltage: V

At 500 V → within ADC dinamic range
G $= e^{\alpha d} \sim 10^4$

* 4 mbar overpressure

padMMe @ CRS: reconstruction

We developed a reconstruction algorithm:

1. **Find the coordinates of the hits →** *X* and *Y* from strip position
   Z from drift time
2. **Clustering the hits in track candidates** (in average 1-2 candidates with 5-6 hits, per view)
3. **Fitting each candidate to find the track parameters →**
   $X = m\,Z + c$
4. **Matching top and bottom planes and x-y views**

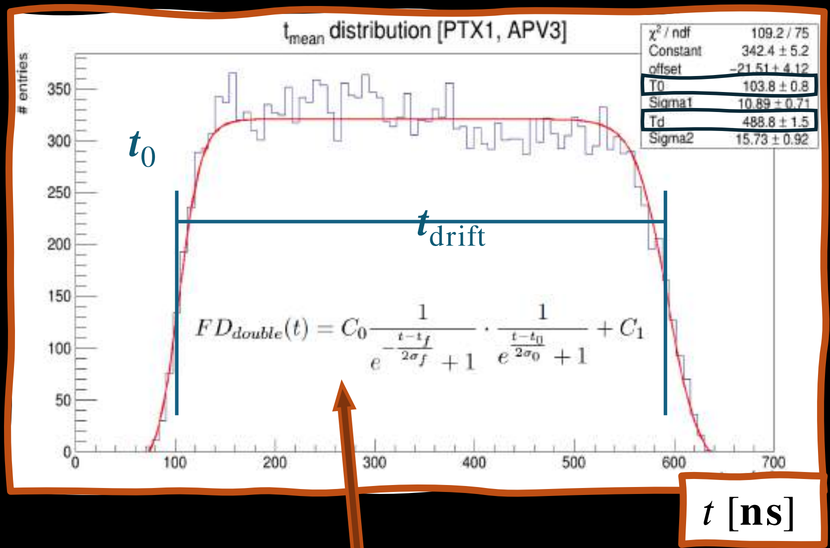

From the hit time distribution, we measured the drift velocity:

$v_{\text{drift}} = d/t_{\text{drift}}$

$v_{\text{drift}} = 10.02 \pm 0.02$ cm/μs

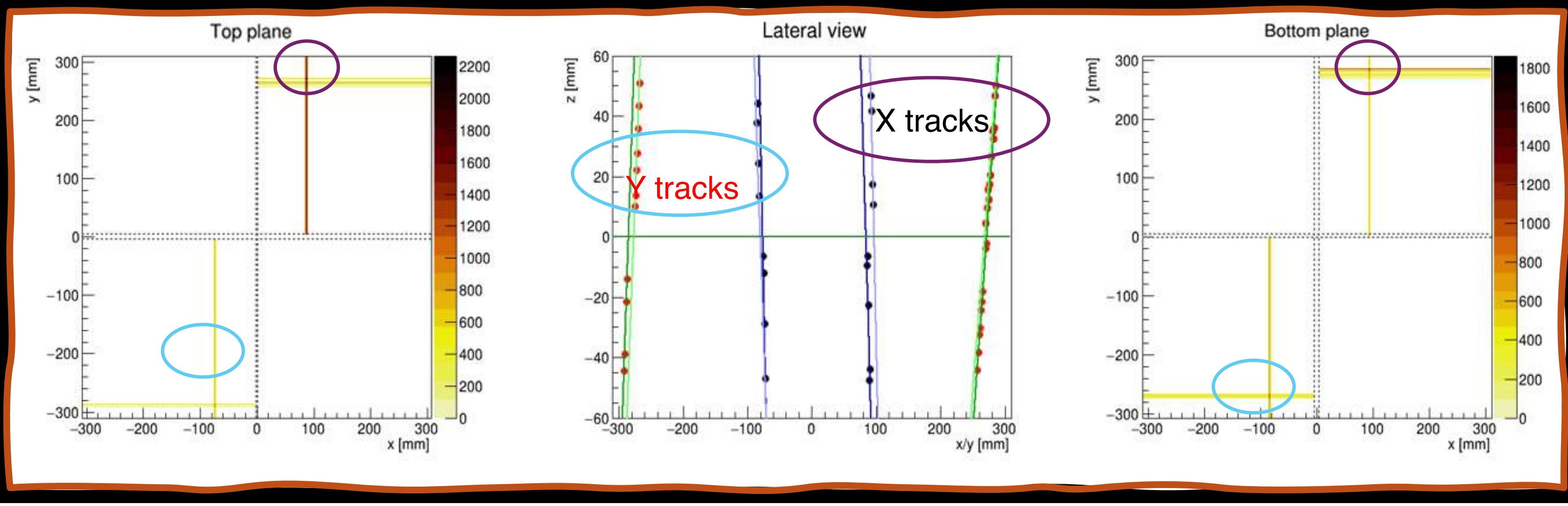

Resolutions@ CRS

From the residues of the track reconstruction we were able to estimate the resolutions:

→ $\sigma_{x/y} \simeq$ 100 µm

→ $\sigma_z \simeq$ 700 µm (and constant with charge!)

→ $\sigma_\theta \simeq$ 7 mrad + 0.2 $|\theta|$

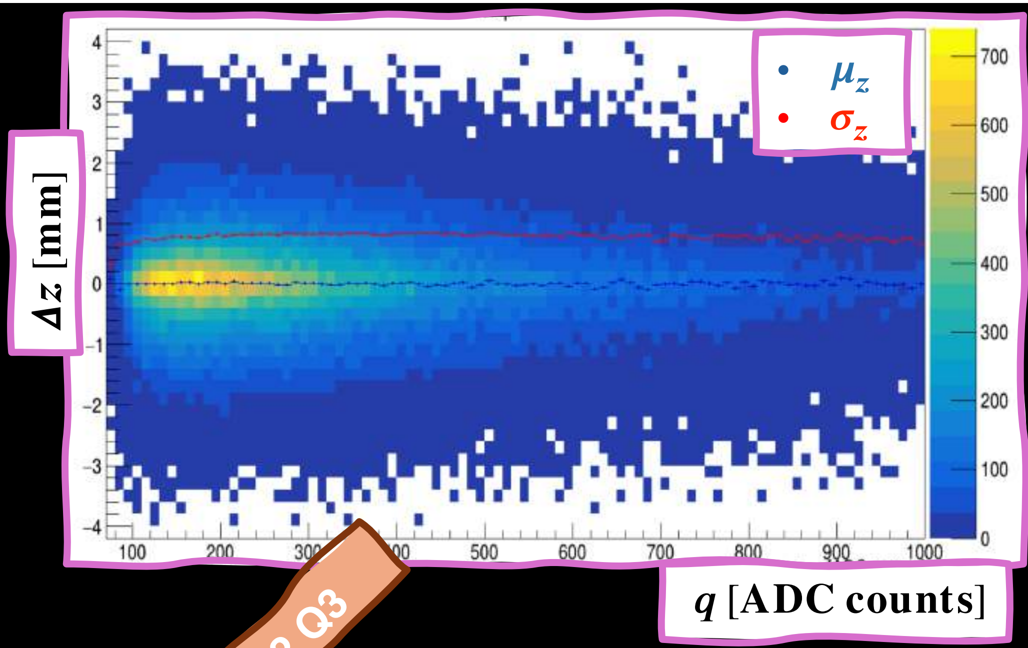

P2 Q3

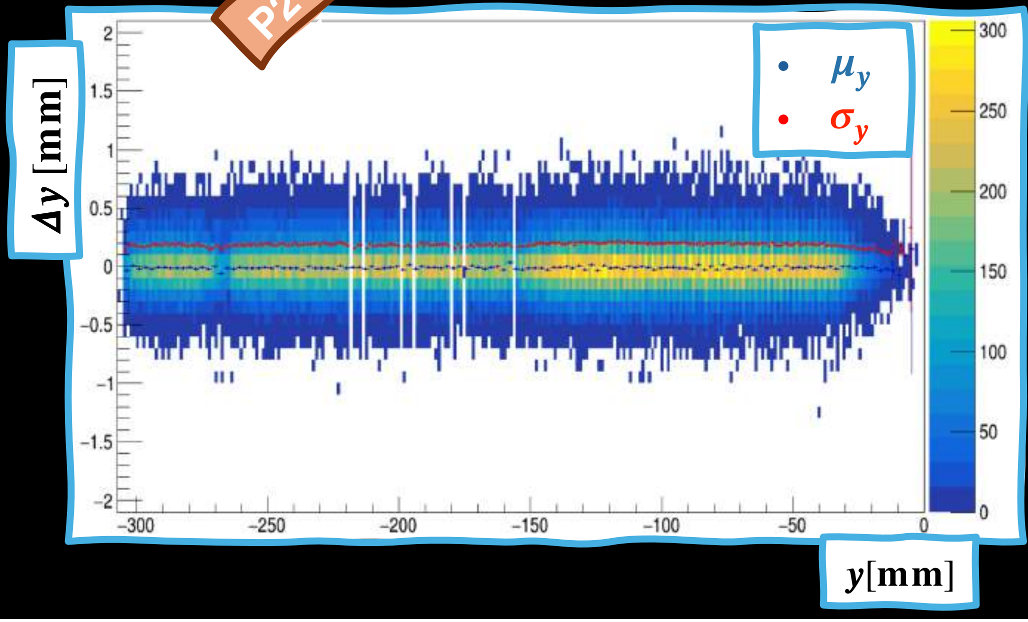

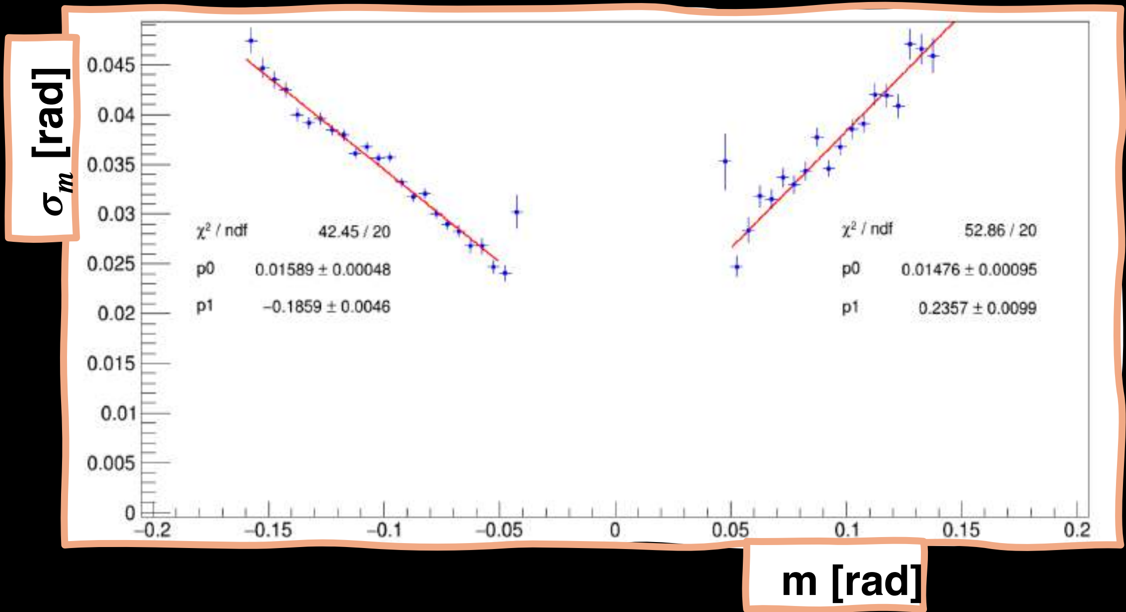

padMMe @ BTF: installation

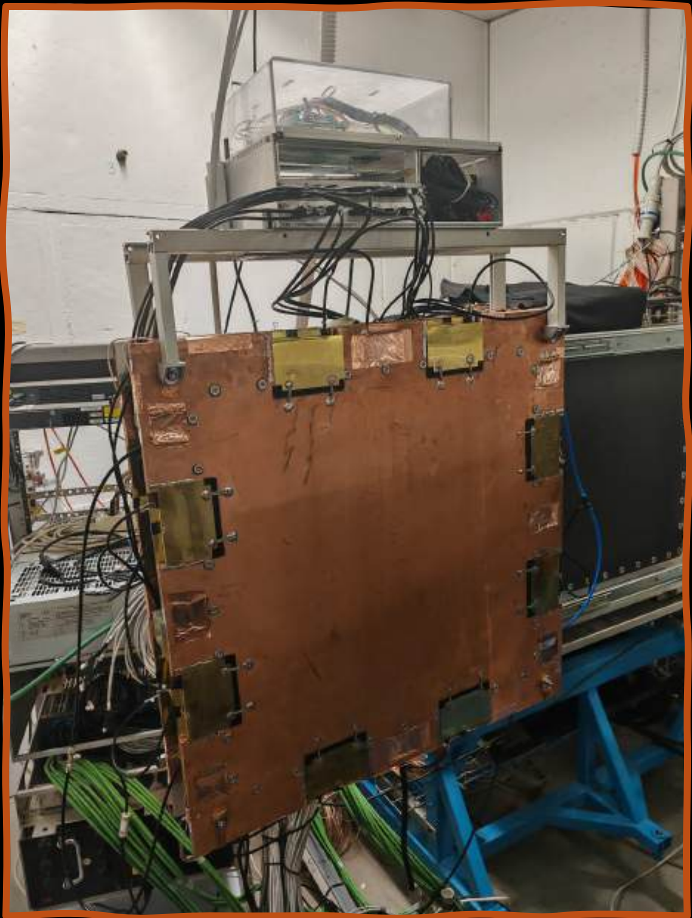

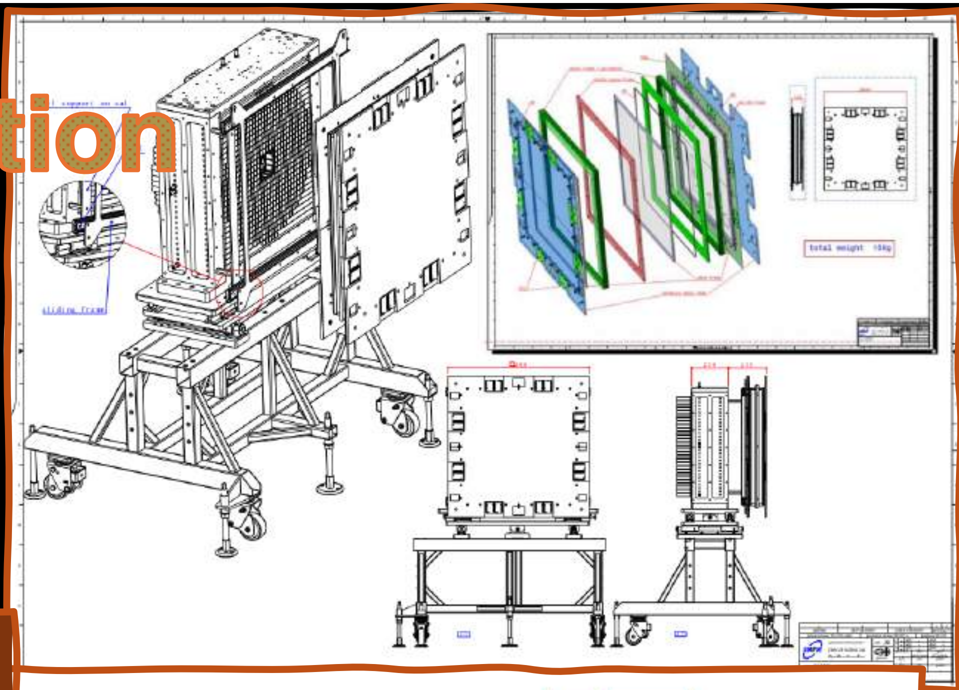

PADME Run IV layout

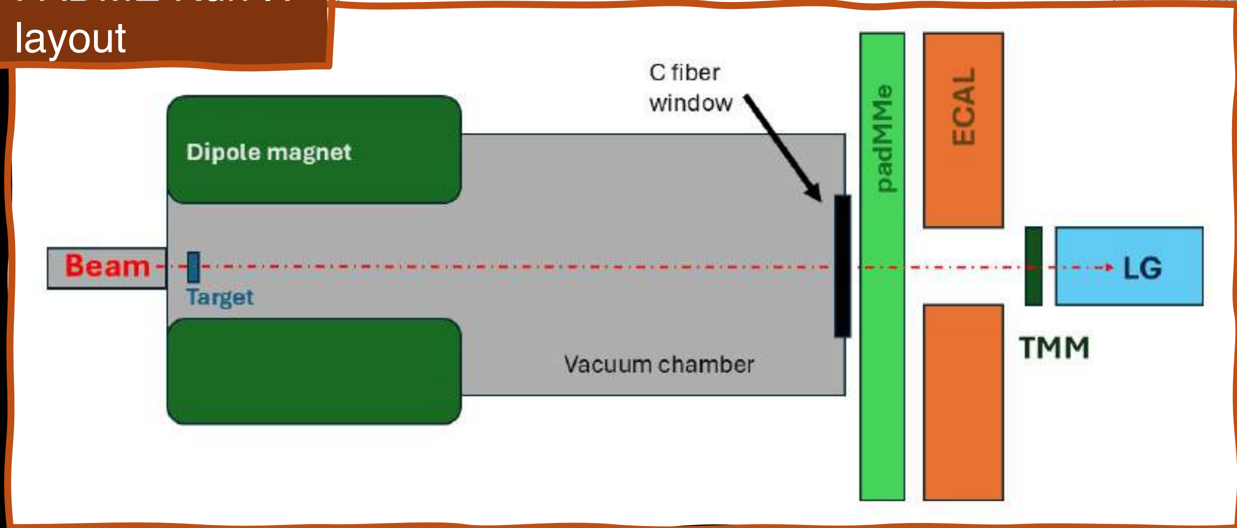

Run IV Data Taking

36 points: Scan 1 and 2 18 points each
~2.2x10^{10} PoT per point
268-295 MeV range, with 0.75 MeV spacing
1 point @ 260 MeV
2 points @ 300 and 330 MeV

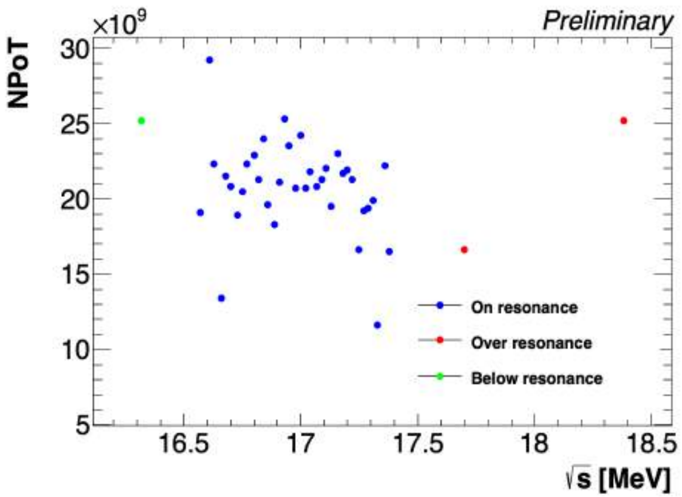

Some online monitoring plots of the data taking

full ECal acceptance available thanks to th target movement

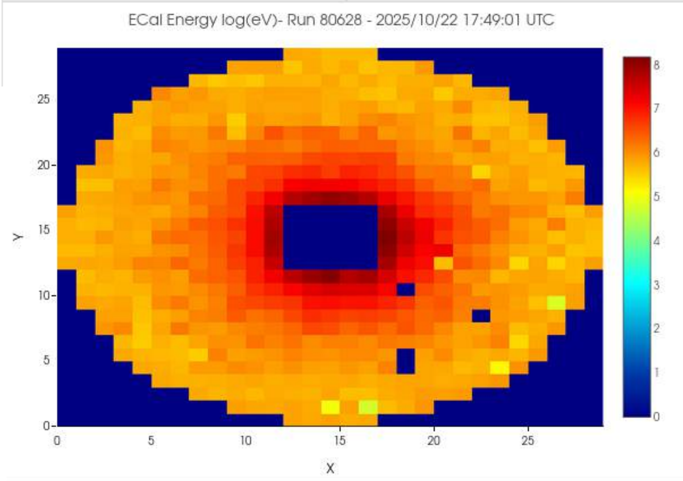

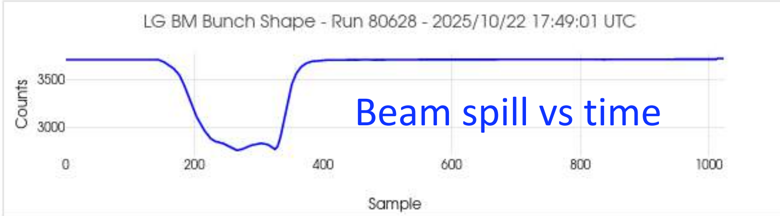

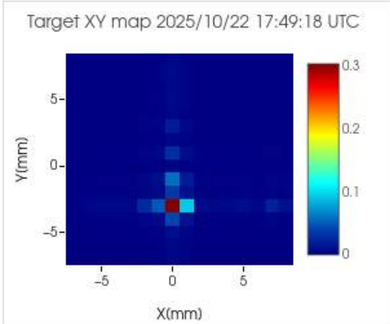

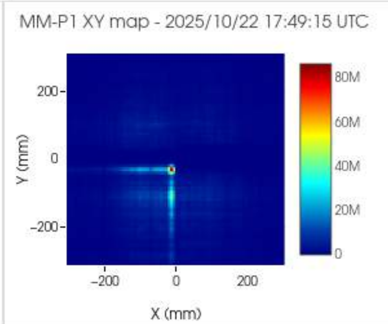

Beam spot @ target

Beam spot @ PadMMe

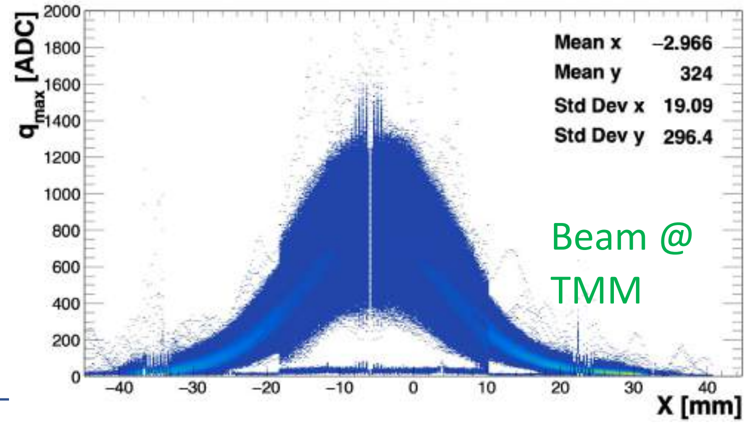

padMMe @ BTF: beam monitoring

Dedicated test runs to check beam monitoring:
- ❖ Inner circle → ionization chamber regime
- ❖ Middle ring → ionization chamber regime

padMMe slightly off-centred to avoid the dead area of the PCB junction.

Measured beam spread: $\sim 5.4 \times 5.4\ \mathrm{mm}^2$

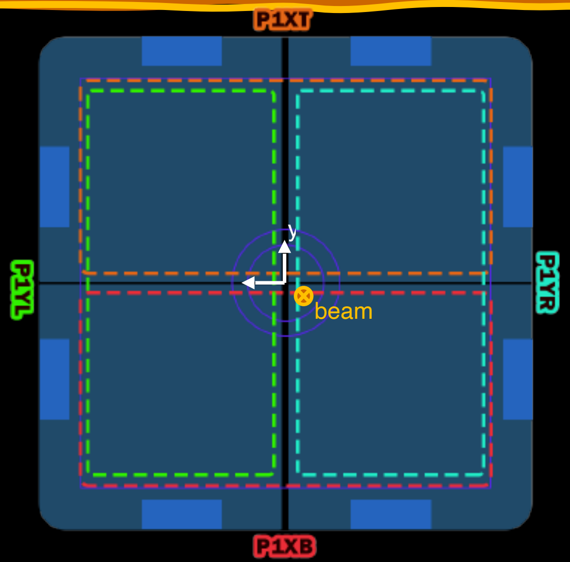

beam position and spread with high precision using padMMe

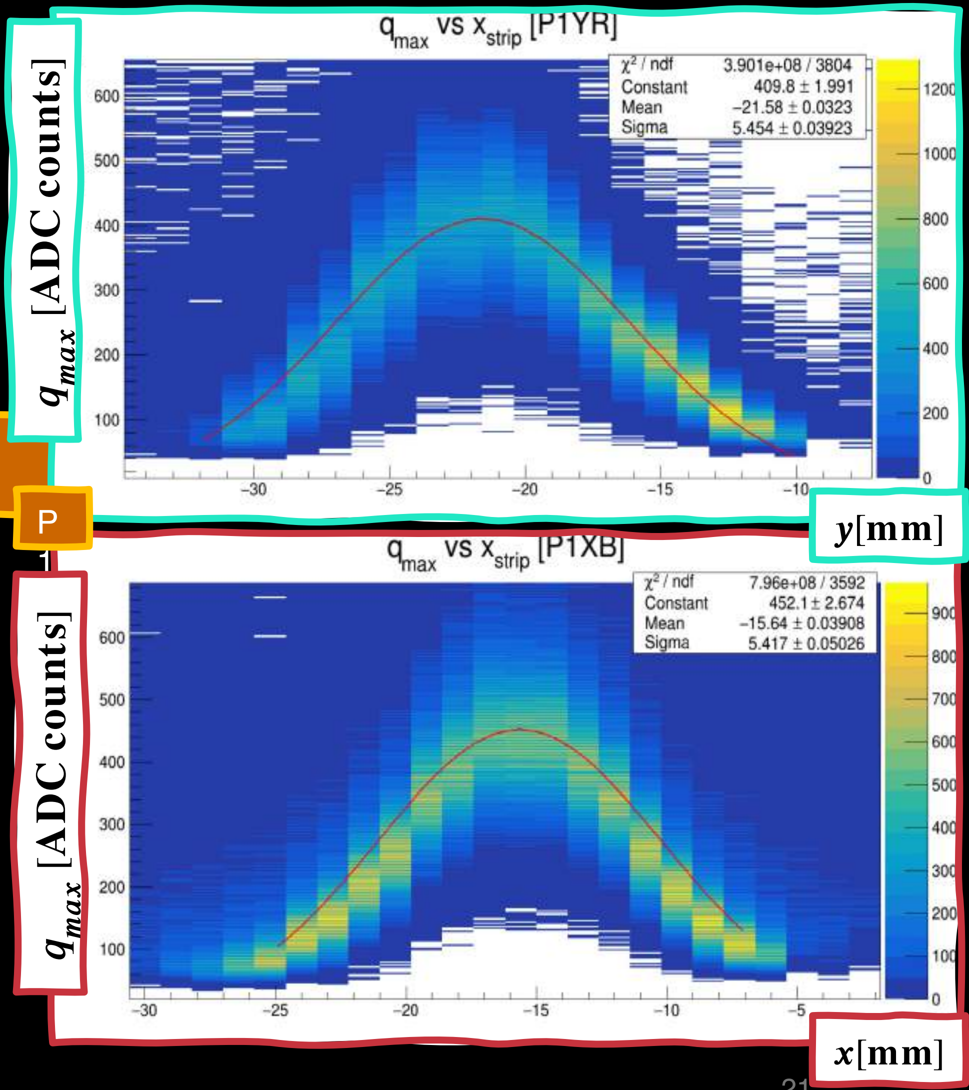

Diamond Target

Target position changed from 3.70 m to 3.36 m

- ϕ_{lab} -cut can be totally removed or adapted
- Acceptance region enlarged → luminosity increases by a factor of 2.5

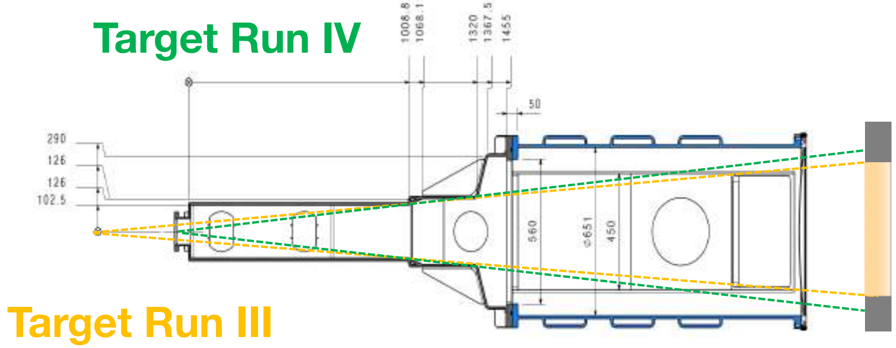

Reconstruction optimization

- Target waveform affected by common-mode noise
  → Average over $\mathcal{O}(100)$ waveforms
- Beam multiplicity $\propto Q = \sum^{t_{stop}} \frac{V(t)}{Z}$

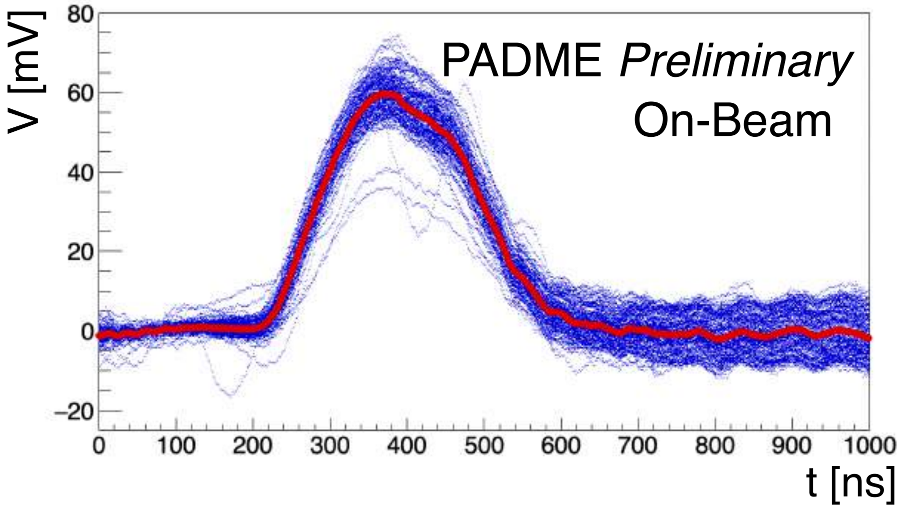

From beam monitors:

target, MM, TMM

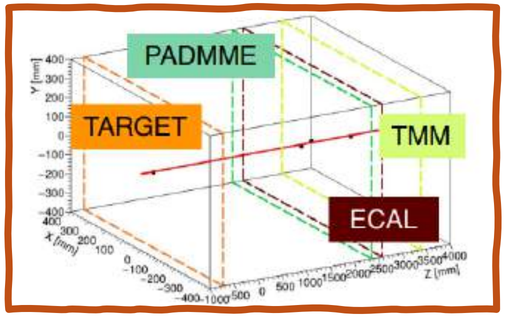

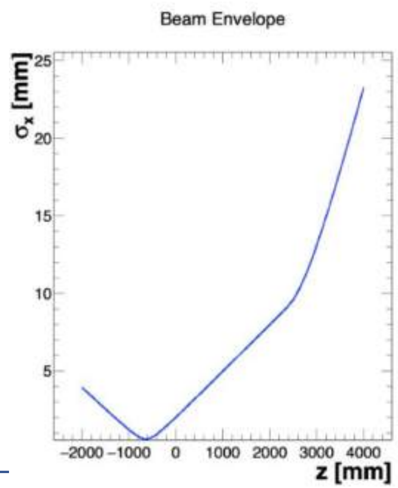

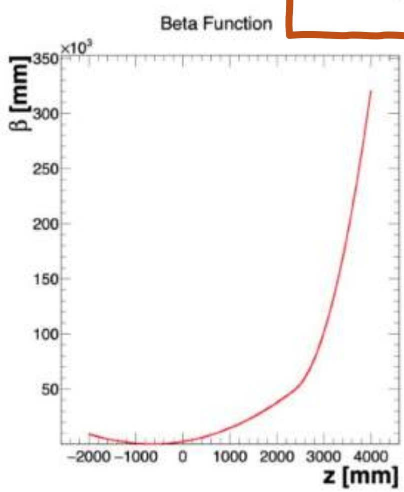


```
===== FIT RESULTS =====
emit  = 1.68892 mm mrad
alpha = 0.509977
beta  = 266.154 mm

===== WAIST =====
Minimum beta = 217.948 mm
Waist position z = -637 mm
```

padMMe @ BTF: commissioning measurements

Beam spread @ padMMe with target in/out the beam line

Having the **beam spread measurement at target and at padMMe** we were able to compute:

Target Multiple Coulomb Scattering

$$\theta^{exp}_{MCS} = \frac{\sqrt{\sigma^2_{target-in} - \sigma^2_{target-out}}}{d_{target-padMMe}}$$

$$\theta^{\mathrm{exp}}_{\mathrm{MCS}} = 0.88 \pm 0.01 \text{ mrad}$$

Beam divergence θ_{div} and **normalized emittance** ε

$$\theta_{div} = \frac{\sqrt{\left(\sigma_x^{padMMe}\right)^2 - \left(\sigma_x^{target}\right)^2}}{d_{target-padMMe}}$$

with target out!

$$\theta_{\mathrm{div}} = 1.08 \pm 0.07 \text{ mrad}$$

$$\varepsilon_{RMS} = \theta_{div} \cdot \sigma_x^{target}$$

$$\varepsilon = \beta\gamma\varepsilon_{RMS}$$

$$\varepsilon = 0.8 \pm 0.2 \text{ mm mrad}$$

padMMe @ BTF: reconstruction

Huge combinatory in pattern recognition (with 3000 e^+/spill)

- ~ 3500/4096 fired strips → ~85% occupancy
- ~200 track candidates found w/o Interaction Point (IP) constraint

→ **IP oriented pattern recognition algorithm**

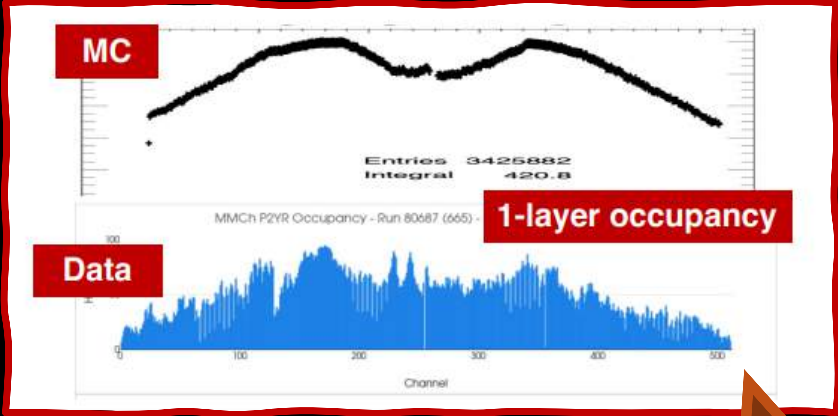

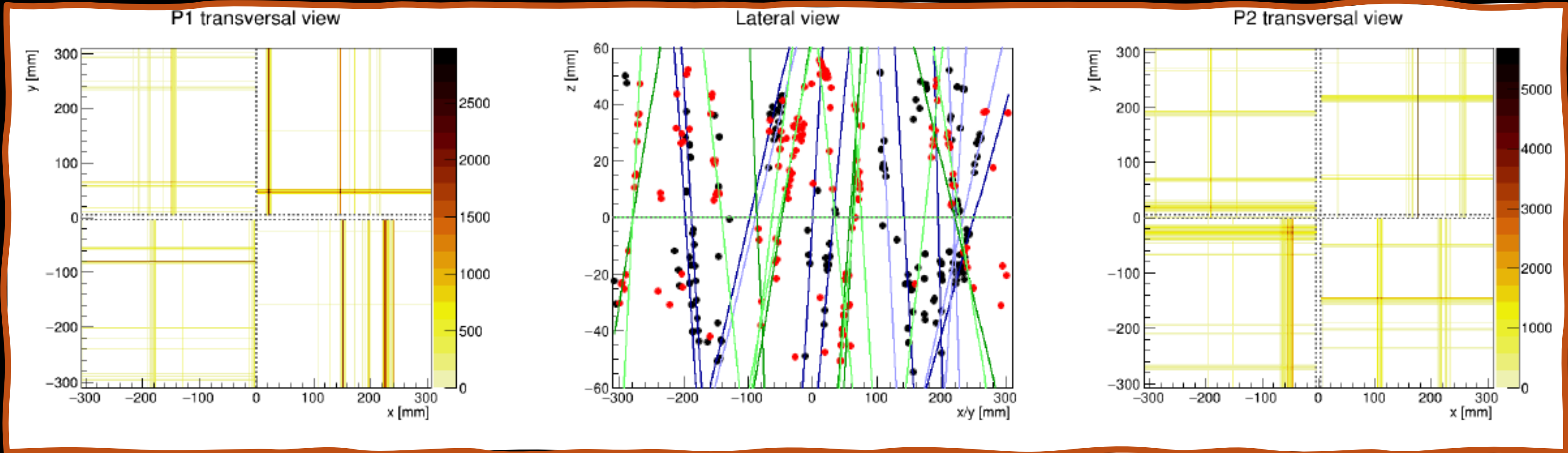

Data and MC simulation agree

padMMe @ BTF: reconstruction

For each charged particle we expect 4 tracks (2D) → **Level-0 tracks**

→ High efficiency but a Level-0 track requirement has high bkg component (combinatorial)

→ **need at least 2/3 out of 4 coincidences**
two-planes coincidence → **Level-1 track**
to be matched with Ecal clusters

Track-to-Ecal-Cluster

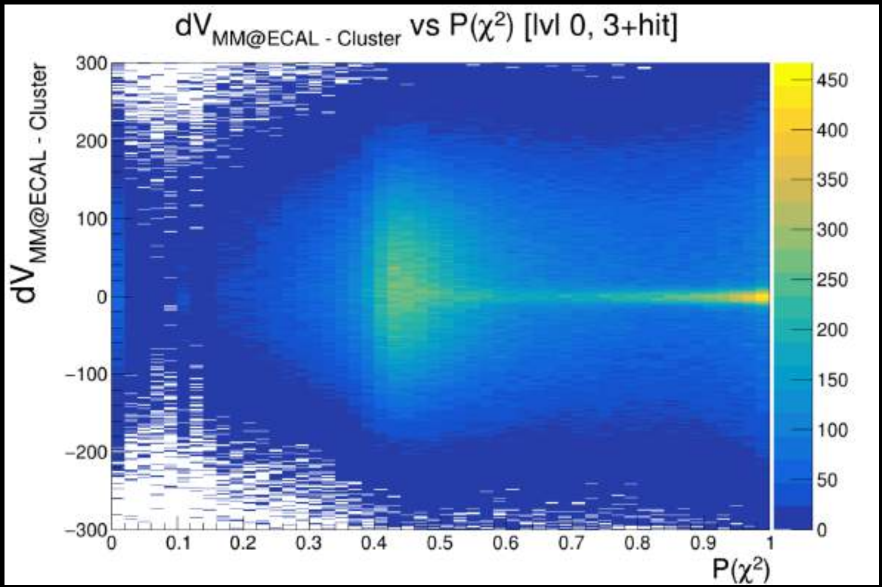

Track direction residuals

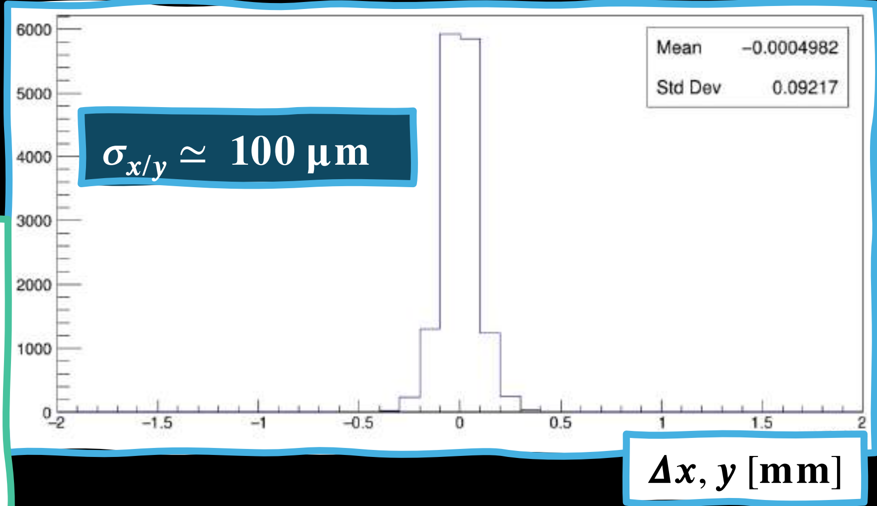

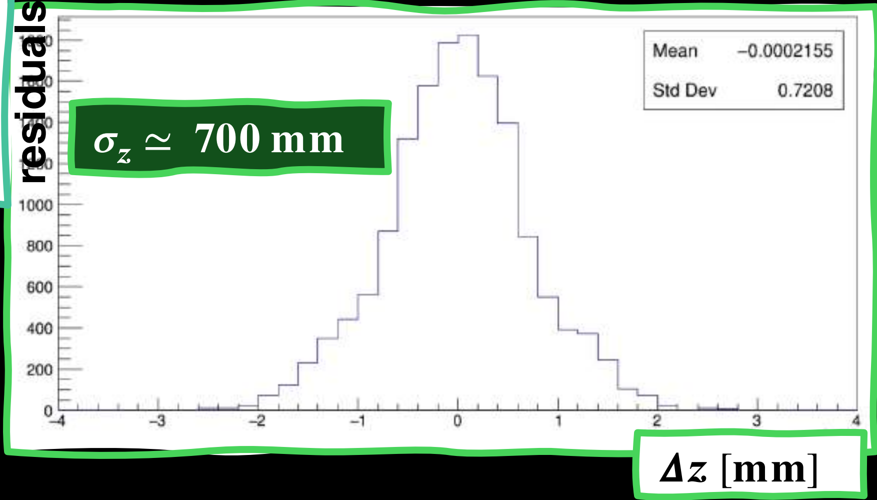

Present performances for beam bkg rejection

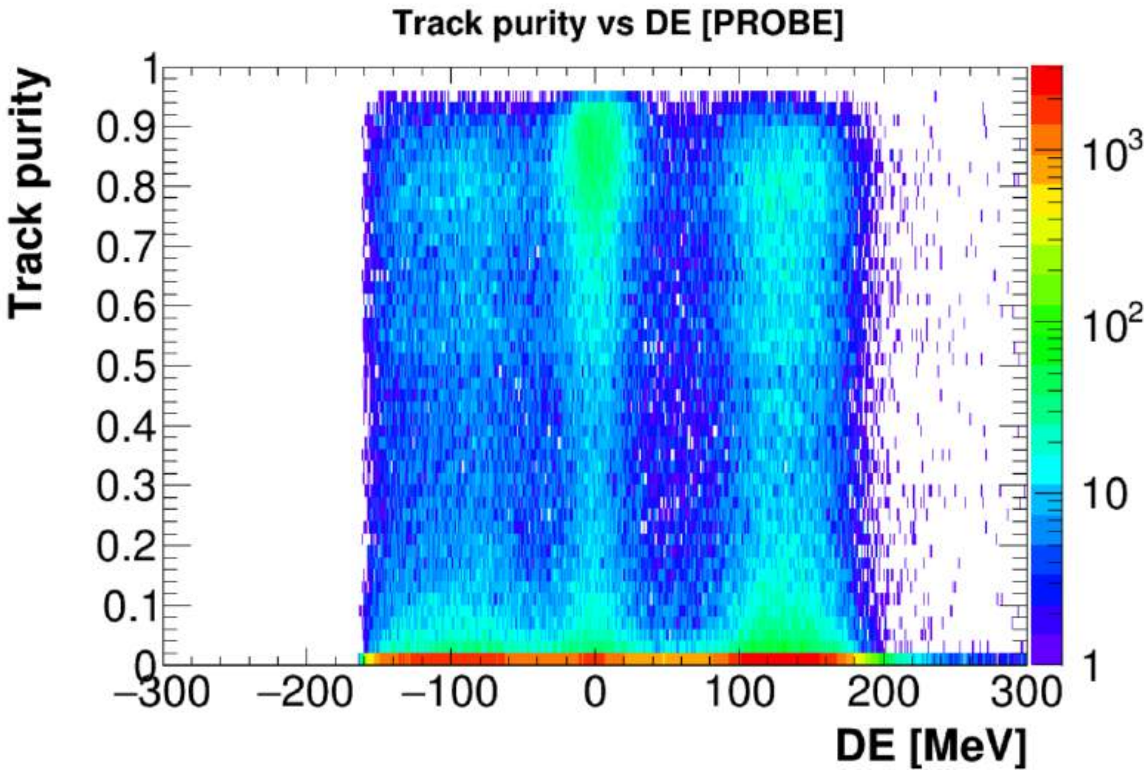

From Bhabha kinematics

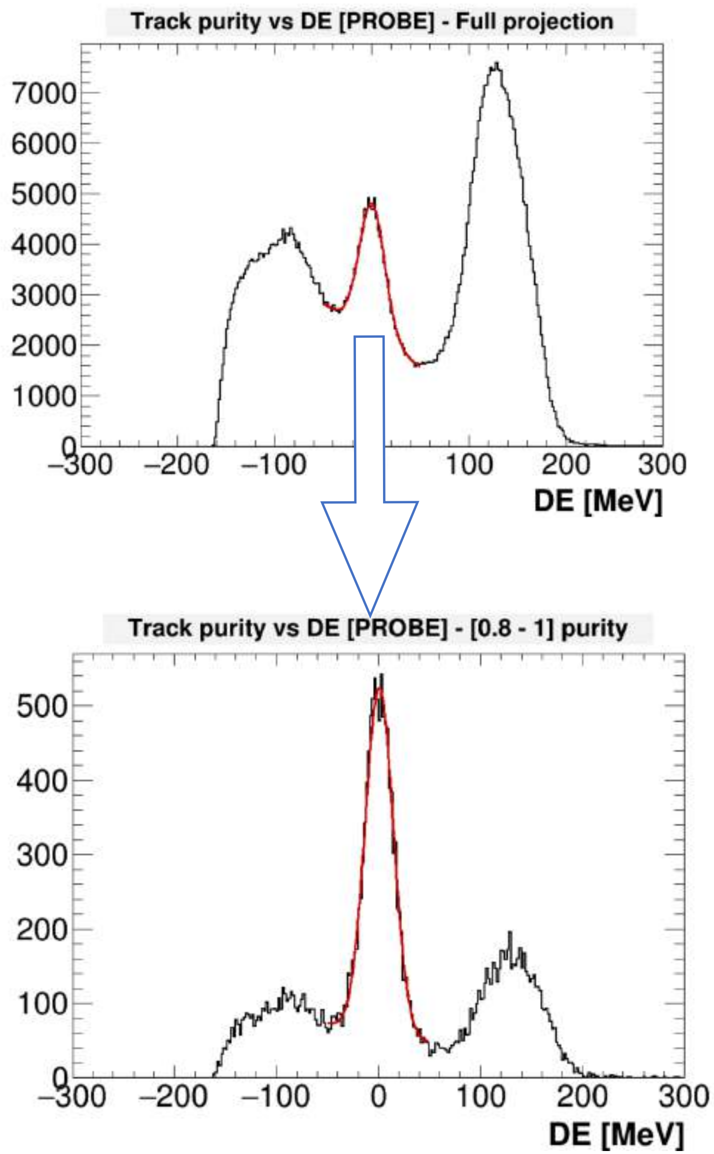

Toward a spectrometer

1

Current Status: X17 resonance search with Beam Energy Scan
→ resolution $O(10^{-2})$, due to beam energy spread and electron motion in the target

Proposal: Final state invariant mass measurement using reconstructed momentum
→ resolution $O(10^{-3})$, completely dependent from tracker

→ Need better tracking performance in magnetic field

2

Make use of angular dependency
→ Need only charge measurement with magnetic field

X17 differential cross section

$$\frac{d\sigma}{d\cos\theta} = \frac{\alpha(s)^2}{4s}\frac{(3+cos^2\theta)^2}{(1-cos\theta)^2}$$

T-channel

$$+\frac{9\,s\,\Gamma_{X_{17}}(s)^2}{4\,m^2}\frac{(1+cos^2\theta)}{(s-m_{X_{17}}^2)^2+s\,\Gamma_{X_{17}}(s)^2}$$

S-channel

$$+\left[(1+cos^2\theta)-\frac{(1+cos\theta)^2}{1-cos\theta}\right]\frac{3\,\alpha(s)\,\Gamma_{X_{17}}(s)}{2\,m}\frac{(s-m_{X_{17}}^2)}{(s-m_{X_{17}}^2)^2+s\,\Gamma_{X_{17}}(s)^2}$$

Interference term

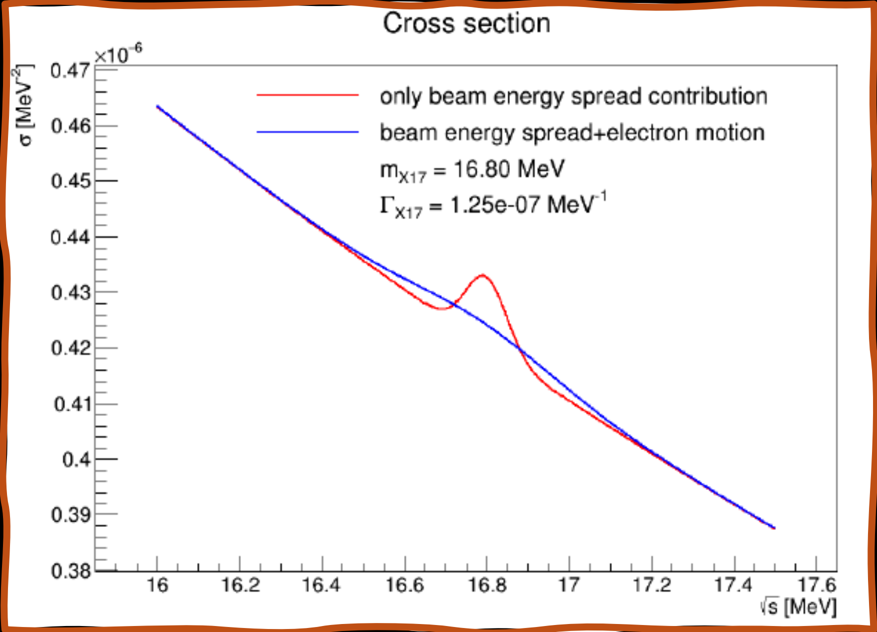

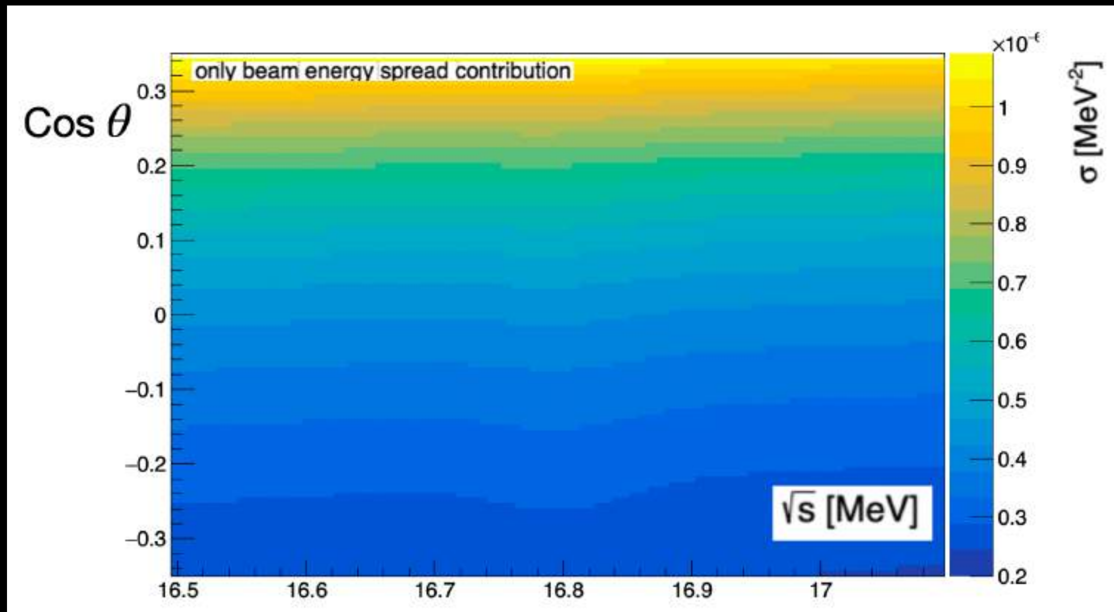

Proposal

New tracker system to be able to measure particle momentum and charge with B field ON

- Current PadMMe does not have enough resolution to get the momentum, and without the magnetic field we cannot measure the charge

- Today able to reconstruct track only with matching with IP due to the high occupancy
  - This match won't be possible with B ON → important to test with B ON to see if we can get rid of low energy particles and reduce the occupancy
  - Beam related backgrounds matters!

New detector requirements

- **Very light** → we cannot go with a multi-layer → one gas gap in TPC mode
  - Current 5 cm gap not enough to measure the momentum because of poor angular resolution
  - Possibly use Helium-based gas mixture to reduce material budget
- **PadMMe-like detector**
  - Only one readout plane close to the calorimeter
  - On the other side possible mylar window (facing the IP side)
- **New detector to measure tracks in the magnet**

Proposal 1: PadMMe-like detector

- Readout plane not instrumented in the beam region (no strip/pad, etc), but mylar window
- Beam bkg much reduced a 1/3 intensity

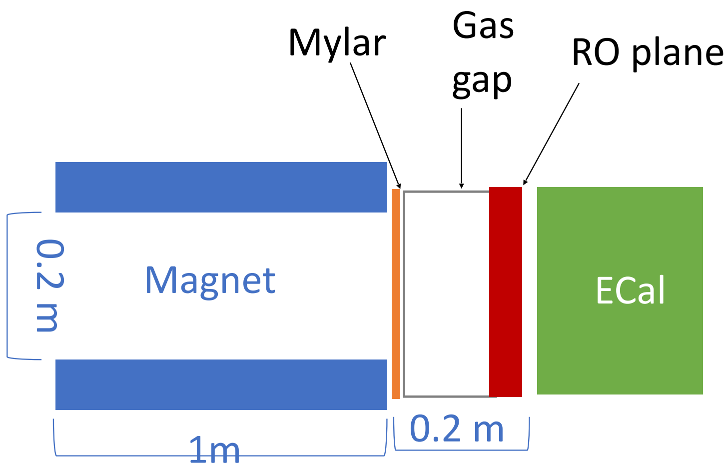

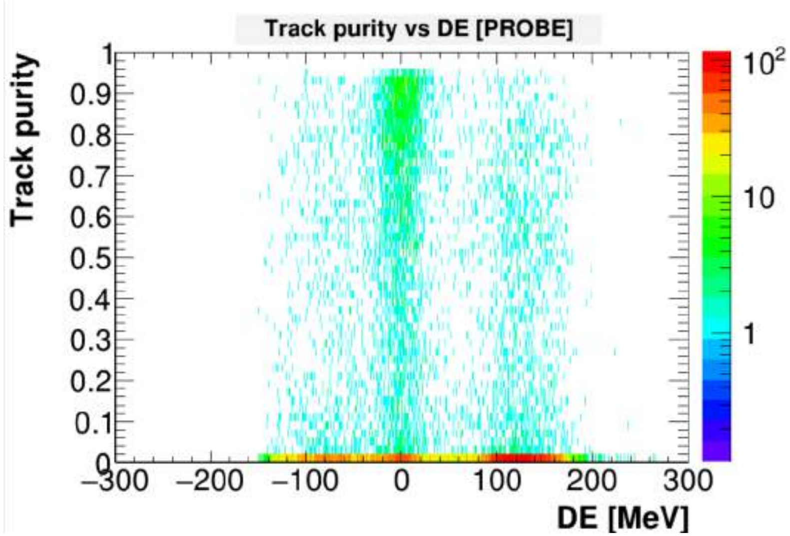

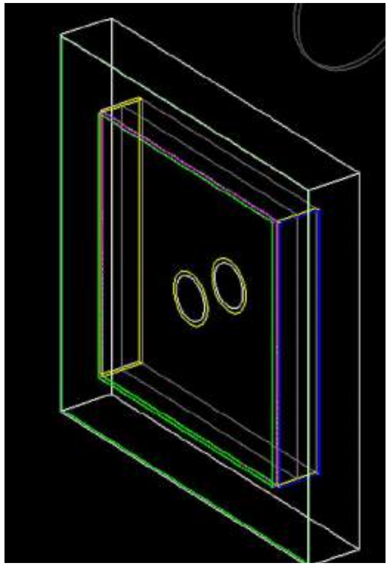

Proposal 2: the “inside” detector

- Detector inside the magnet
  - Same dimension of the magnet
  - 2 “mylar” window at the edges (of course we need gas tightness and interface with target region and the other tracker)
  - 1 readout plane on the bottom
- Readout Layout Pad-based
  - We need to measure the particle trajectory on the bending plane (where is the readout now)
  - Segment the bending plane in limited z sections (~10) to lower the readout channels

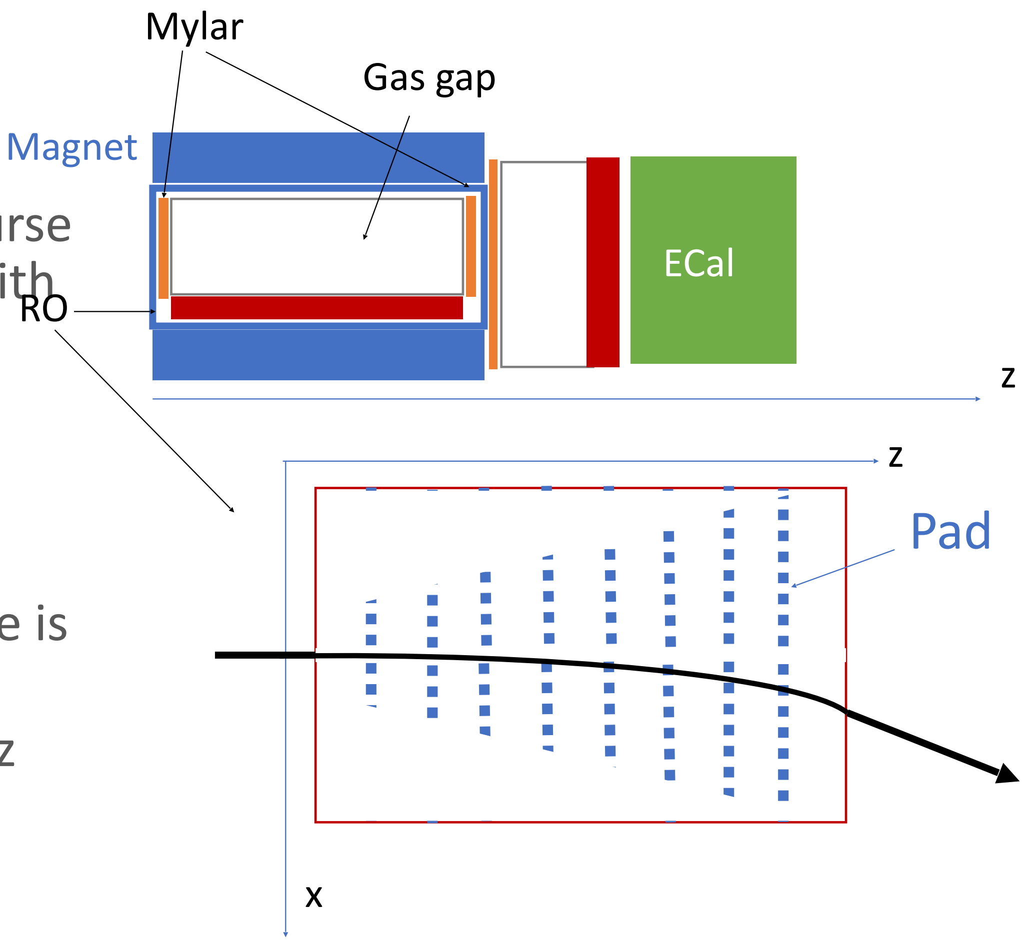

Readout & DAQ

- Current setup with APV limited in time window due to sampling→ not possible to measure 20 cm drift time
- **Proposal 1**: Modify the current firmware in a way that it acquire “continuously”: determine charge and time @ FPGA level
  - Pros: we already have the APV
  - Cons: require changes in the firmware and on MMDaq
- **Proposal 2**: use of the VMM3 → ADC+TDC embedded in the FE, no limit in time window acquisition
  - Pros: Support from the community (DRD1/ATLAS), working setup possibly available at CERN and join next Test Beam in July to test a prototype setup
  - Cons: Need to buy new full set of electronics

Conclusions

The **Run III** data analysis shows an excess @ 16.9 MeV, with global p-value equivalent to 1.8(2)σ

- Overall uncertainties ~ 0.9% per energy point
- No indications of X17 well beyond 2σ-equivalent global p-values

The **Run IV** data needed to clarify

- Improve sensitivity (higher statistics and better control of systematics) aiming at a factor of 2 error reduction
- New Micromegas tracker were installed to measure the absolute ee/$\gamma\gamma$ cross section allowing combined analysis
- Redundant beam parameter measurements also with TMM to the end of the line for beam monitor
- Signal yield increased by a factor of ~ 2.5 wrt Run III

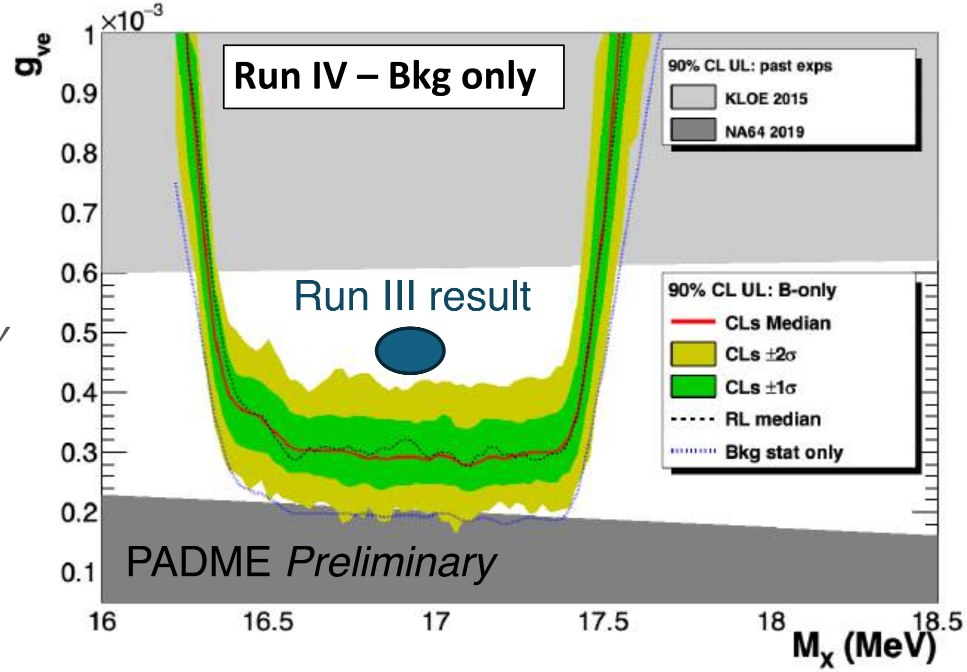

On the basis of the ongoing analysis of Run IV and during the test runs, we are currently evaluating the possibilities to significantly increase the sensitivity of the experiment in future running campaign

(using lighter materials for target, reduce passive material in the tracker to mitigate multiple scattering)

Run III: analysis & results

Run III features:

- Intrinsic width ~ eV or smaller (from ATOMKI) while experimental width ~100 keV ($\sqrt{s}$ spread)
  → $\sqrt{s}$ scan in steps of 30 keV , between [16.4 MeV – 17.4 MeV] ← → [262 MeV – 296 MeV] beam energy
- Vector boson hypothesis → coupled to EM current
- Comparison of signal hypothesis vs SM background:

$$N_{2cl}(s) = N_{POT}(s) \times [\, B(s) + S(s; M_X, g)\, e_S(s) \,]$$

vs

$$N_{2cl}(s) = N_{POT}(s) \times B(s)$$

→ Found excess at $m_x c^2 = (16.90 \pm 0.02)$ **MeV**

$g_{ve} = 5.6 \times 10^{-4}$, $\Gamma_{exp} \sim 100$ keV

corresponding to local 2.5σ

global (1.77 ± 0.15) σ one-side

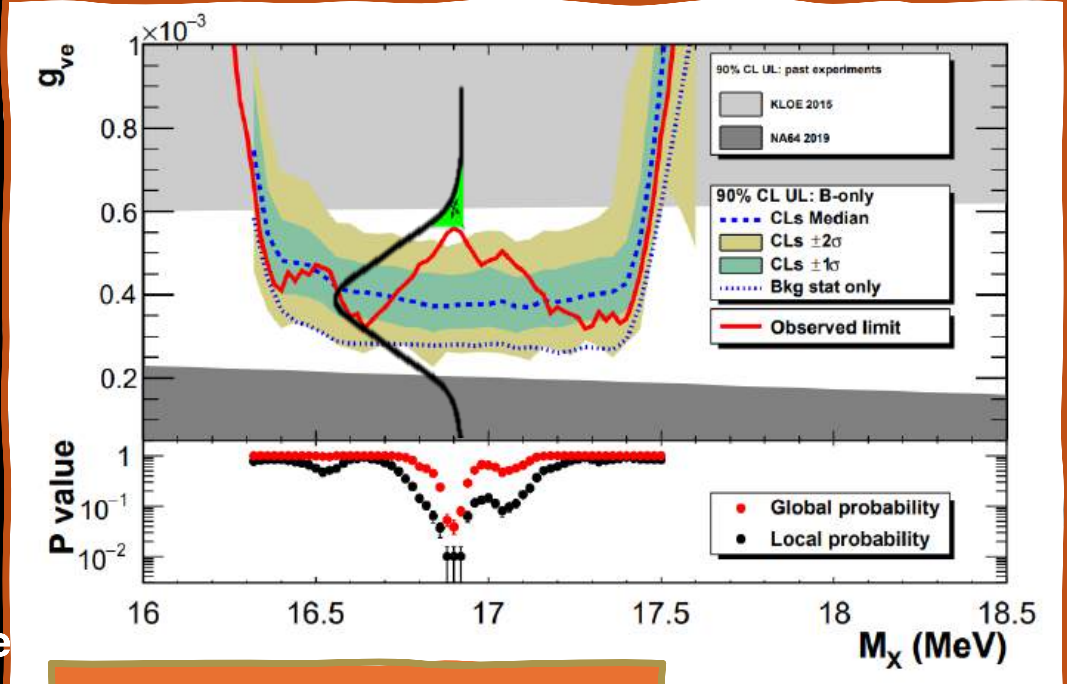

DOI: 10.1007/JHEP11(2025)007

padMMe: dimensional measurements

PADME

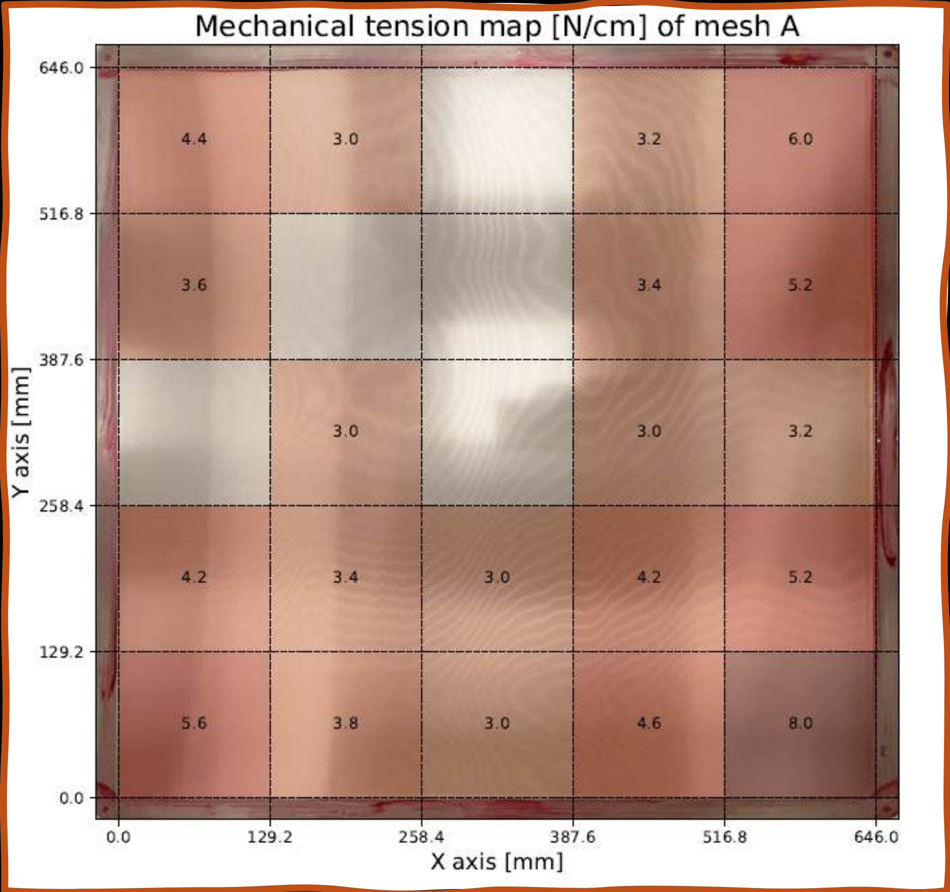

Pillar height

padMMe: deformation of readout panel

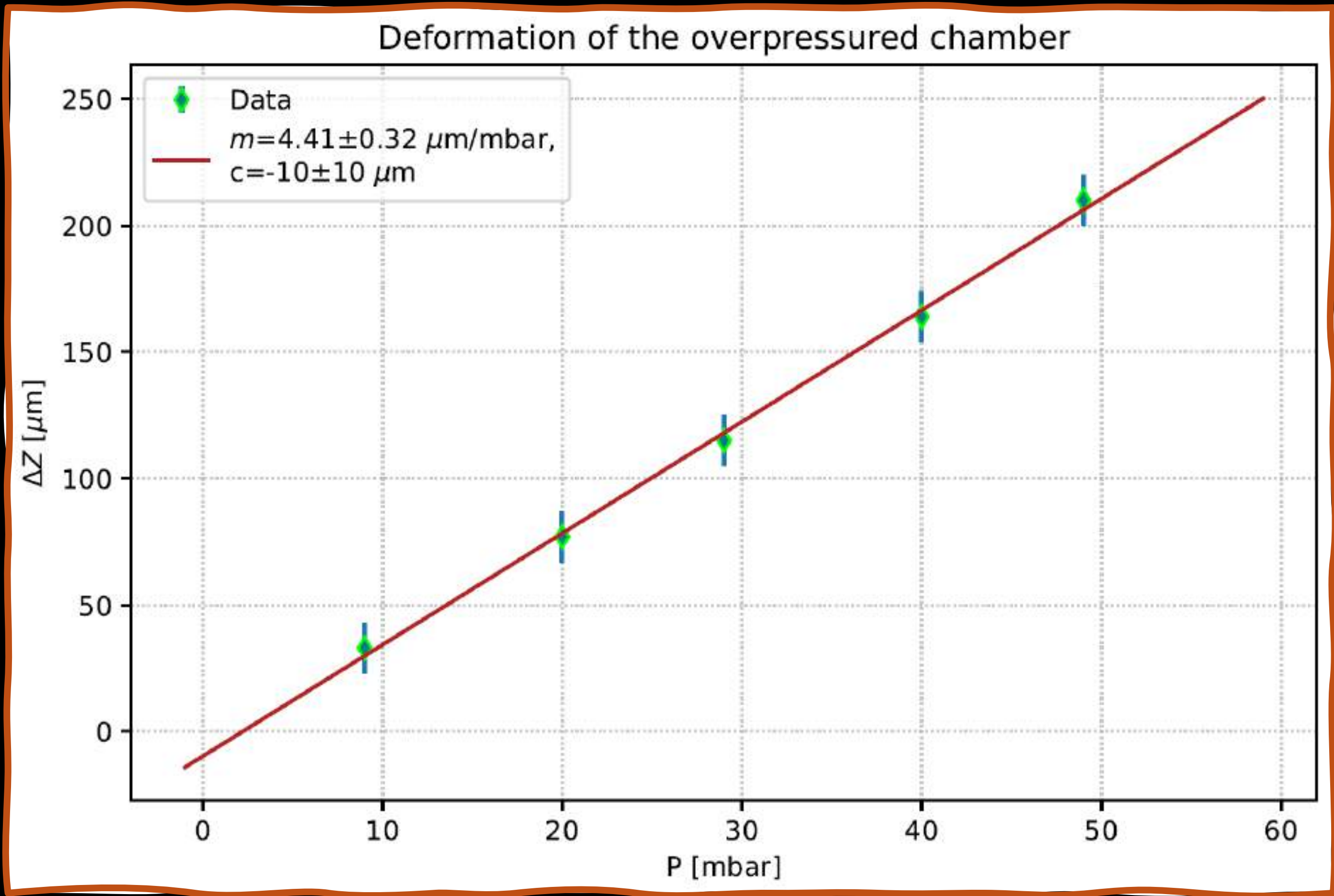

padMMe: gas tightness

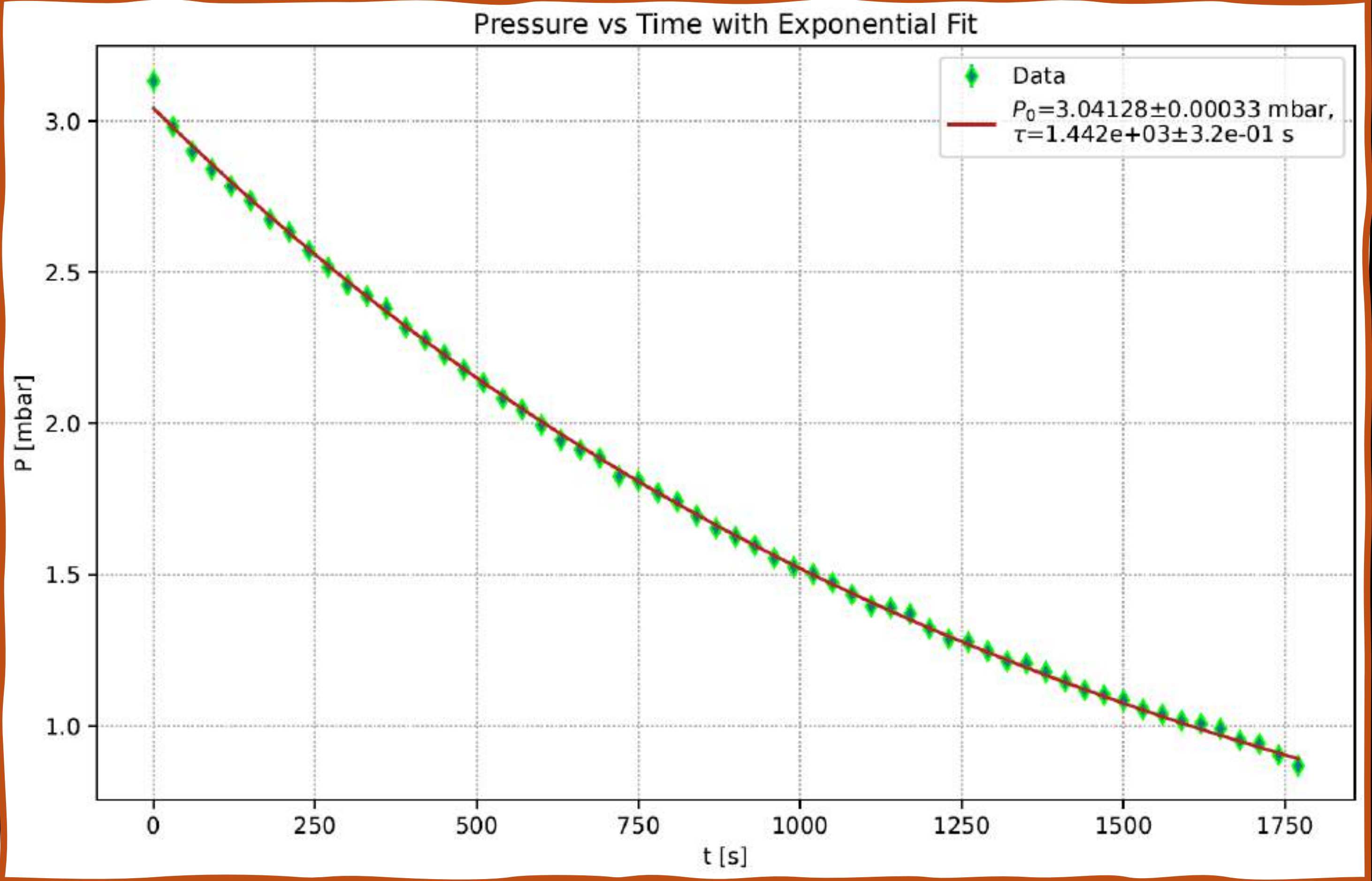

Time of

$$\tau = (1442.00 \pm 0.32)\ \mathrm{s} \simeq 24\ \mathrm{min.}$$

Volume leakage:

$$\frac{V}{\tau} = (0.8989 \pm 0.0020)\ \mathrm{L/h}$$

padMMe @ CRS: reconstruction

$$X \text{ or } Y = \#ch * p + \Delta_{sectors}$$

$$t_{drift} = t_{mean} - t_0$$

Mean time of the signal (charge-weighted average)

From time calibration

$$\text{TOP panel:} \quad Z = d - Z_{corr} - t_{drift} \cdot v_{drift}$$
$$\text{BOTTOM panel:} \quad Z = -d + t_{drift} \cdot v_{drift} + Z_{corr}$$

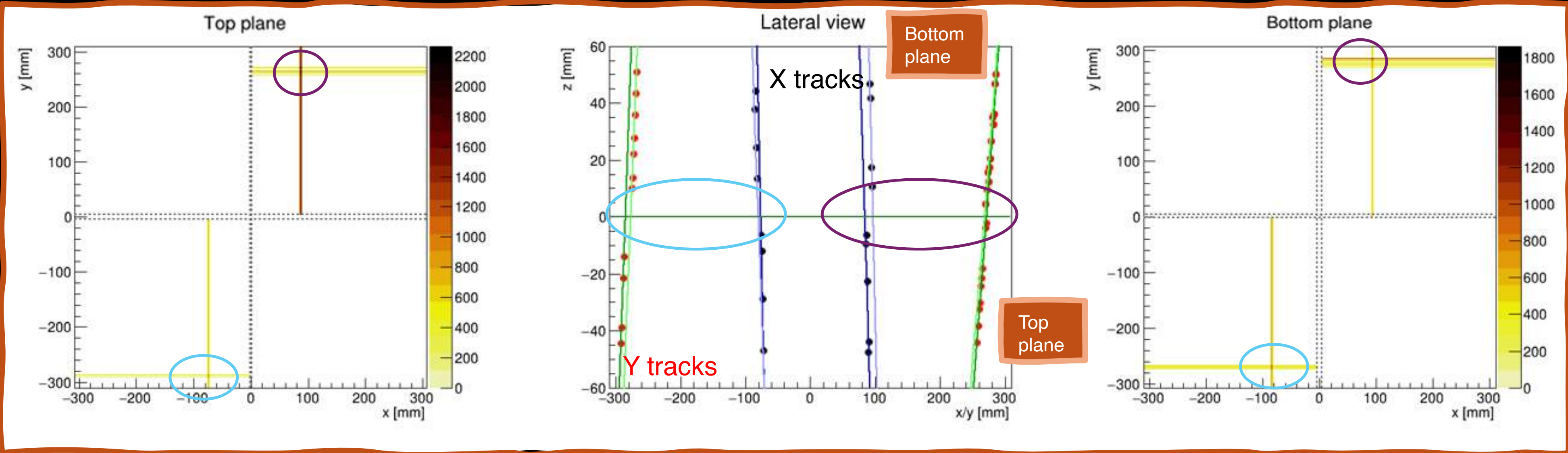

Event selection

Estimation of N_2

Selection algorithm as independent as possible on beam and detector conditions

- Require 2 clusters within ECal geometric acceptance
  - R_{max} defined by ECal dimensions and R_{min} by the CoM energy
  - Limited energy range for each cluster, depending on CoM energy
  - Illumination affected by the presence of the magnet → Cut regions in φ
    - about 30% loss in acceptance
- Mutual cluster conditions
  - Time and spatial distance: $\Delta T < 5$ ns & $\Delta R > 60$ mm
  - $\phi 1 - \phi 2$ vs $\theta 1 + \theta 2$ cut in the center of mass frame isolates the signal
    - → Signal Region is 3σ around the mean value
    - → Sideband Region to determine background normalization
  - ~ 4% originating from Bremsstrahlung radiation in the target subtracted to obtain the final N_2 estimation

Source of uncertainty	Error on N_2 [%]
Statistics	0.6 – 0.7
Background subtraction	0.3
Total (uncorrelated)	0.65

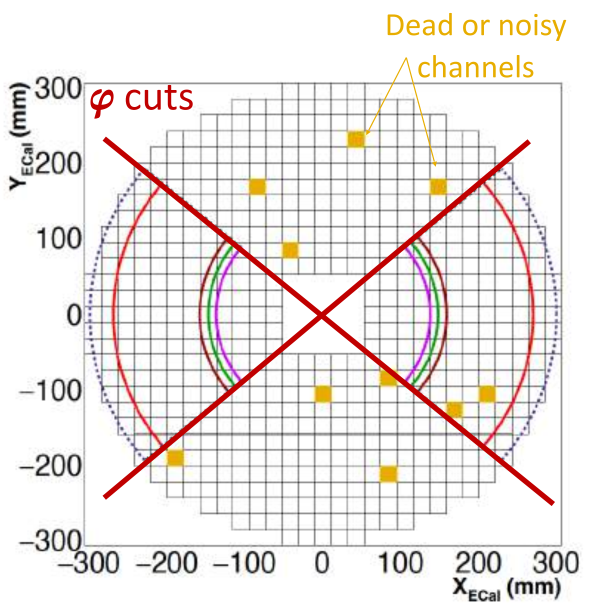

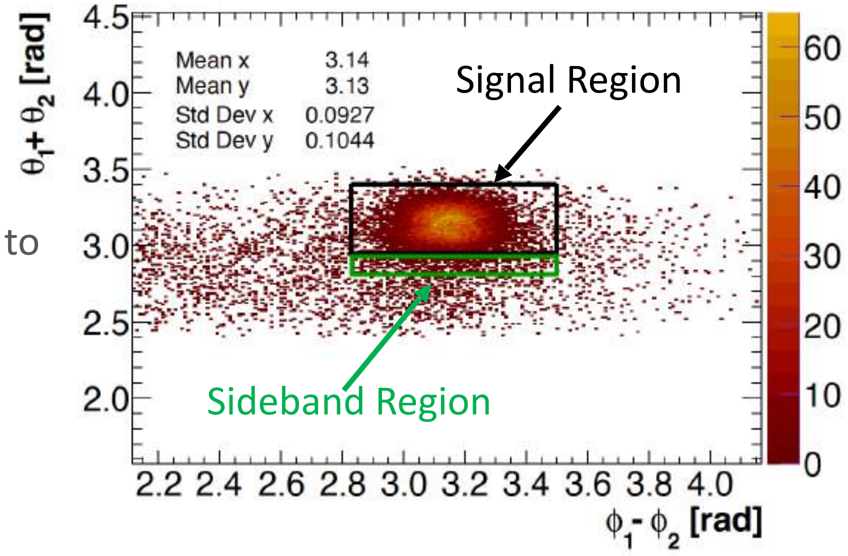

SM Background

Estimation of B

The main background sources are the Bhabha scattering and $\gamma\gamma$ annihilation.

The expected background yield per PoT is determined with MC → validate with data

- Reconstruction efficiency estimated with Tag&Probe method → data/MC compatible with 1

Effects that spoils the B estimation:

- Beam spot direction & shape → acceptance variation of 0.08% - 0.1%/ mm of vertical shift
- Stability of cuts due to acceptance edge effects and leakage → estimated by varying R_{max}

Tag & Probe efficiency

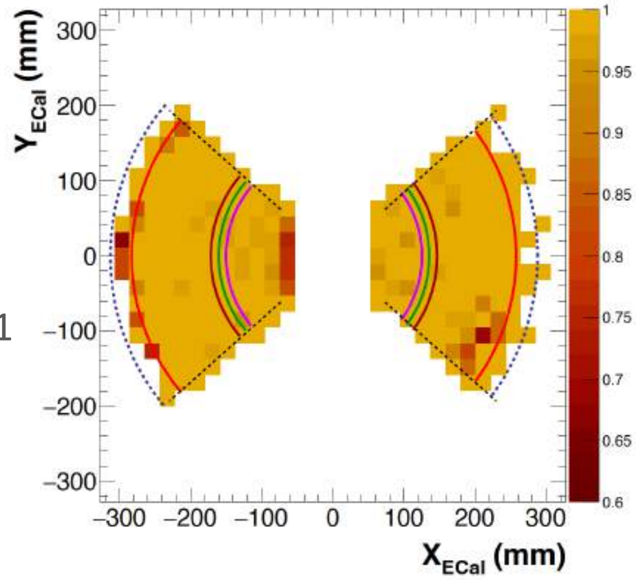

Source of uncertainty	Error on B [%]
MC statistics	0.4
Tag & Probe eff.	0.35
Beam spot variations	0.05
Cut stability	0.04
Total (uncorrelated)	0.54
Absolute B yield (correlated, affect K(s))	1.8

B yield normalized to below-resonance energy points
→ improve systematic uncertainty

Radiative corrections
e+e-(γ) and $\gamma\gamma$(γ)
evaluated using BabaYaga
→ 3% decrease in the total cross section @ 16.92 MeV and a √s slope of -0.6(6) % MeV^{-1}

Radiative Corrections

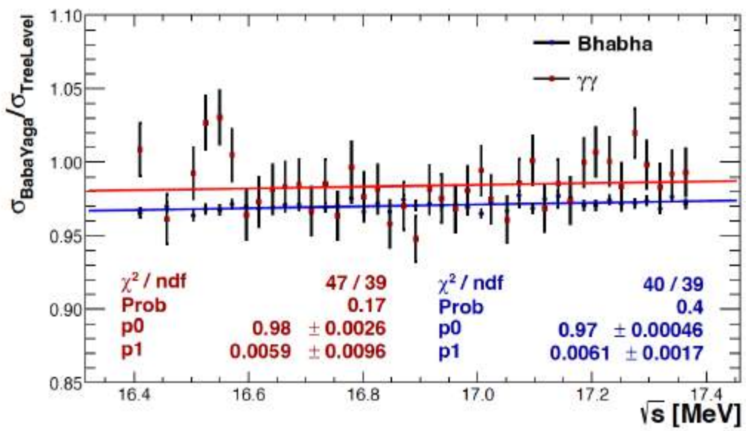

Positron on target

Estimation of N_{PoT}

The number of PoT per bunch is determined using the LeadGlass calorimeter charge.

$$N_{PoT} = \frac{Q_{LG}}{Q_{1e^+,402\,[MeV]}} \times \frac{402}{E_{beam}[MeV]}$$

Radiation induced loss

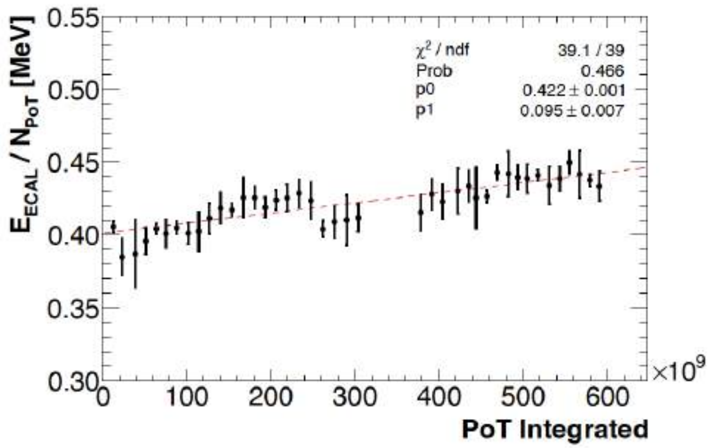

Energy loss in passive material

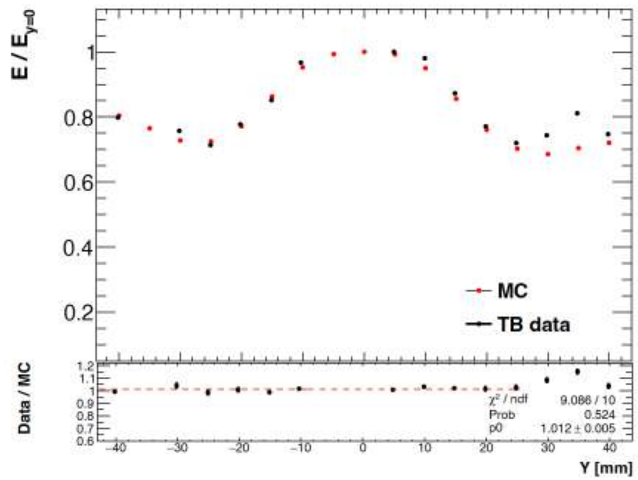

Corrections for precise estimation of N_{PoT}

- Radiation induced loss
  - Run III dose ~ 2.5 krad → transparency changes for O(krad)
  - Estimated from 2 flux proxy observables: Q_{target} , E_{ECal}

    → show a linear energy dependence on the integrated flux → LG yield decreases by 0.097 ± 0.007 → N_{PoT} flux corrected for this effect
  - Error associated both to the constant term and to the slope of the correction
- Energy loss in passive material
  - Beam movements → passive material crossing (TimePix cooling system)
  - Test beam to check goodness of MC simulation → evaluate the overall energy loss for the specific beam conditions → for each energy point N_{PoT} flux corrected

Source of uncertainty	Error on N_{PoT} [%]
Radiation Loss. slope (uncorrelated)	Variable ~ 0.35
Common errors on N_{PoT} (affect K(s))	
LG Calibration pC/MeV	2.0
Energy Loss	0.5
Radiation Loss, const. term	0.3
Total (correlated)	2.1

Signal modelling & efficiency

Estimation of S and ε_{Sig}/B

Signal yield estimation

The width of the expected excess receive contributions by the beam energy spre
and from the electron motion in the target.

- Functional form is a Voigt distribution parametrized as function of the beam energy: convolution of the Gaussian for the BES with a Lorentzian

→ Uncertainty in the curve parameters as nuisances:

  - Lorentzian width around the resonance energy: 1.72(4) MeV
  - Relative BES: 0.25(5)%

Signal efficiency

Expected signal efficiency ε_{Sig} determined from MC:

- Use of the ratio ε_{Sig}/B significantly reduces detector-related systematic uncertainties (similar detector illumination for both signal and background).

→ Fit ε_{Sig}/B with a straight line → fit parameters as nuisances:

  - Errors: ΔP0/P0 ~0.1%, ΔP1/P1 = 3%, correlation = -1.8%

[12] Phys. Rev. Lett. 132 (2024) 261801